Title

Estimation of the receptor-state affinity constants of ligands in functional studies using wild type and constitutively active mutant receptors: Implications for estimation of agonist bias

Authors

Ehlert, Frederick J
Stein, Richard SL

Publication Date

2017

DOI

10.1016/j.vascn.2016.09.007

Peer reviewed

HHS Public Access

Author manuscript

J Pharmacol Toxicol Methods. Author manuscript; available in PMC 2018 January 16.

Published in final edited form as:

J Pharmacol Toxicol Methods. 2017 ; 83: 94–106. doi:10.1016/j.vascn.2016.09.007.

Estimation of the receptor-state affinity constants of ligands in functional studies using wild type and constitutively active mutant receptors: Implications for estimation of agonist bias

Frederick J. Ehlert[a,b,*] and **Richard S.L. Stein**[b]

[a]Department of Pharmacology, School of Medicine, University of California, Irvine, Irvine, CA 92697-4625, United States

[b]Department of Anatomy and Neurobiology, School of Medicine, University of California, Irvine, Irvine, CA 92697-4625, United States

Abstract

We describe a method for estimating the affinities of ligands for active and inactive states of a G protein-coupled receptor (GPCR). Our protocol involves measuring agonist-induced signaling responses of a wild type GPCR and a constitutively active mutant of it under control conditions and after partial receptor inactivation or reduced receptor expression. Our subsequent analysis is based on the assumption that the activating mutation increases receptor isomerization into the active state without affecting the affinities of ligands for receptor states. A means of confirming this assumption is provided. Global nonlinear regression analysis yields estimates of 1) the active (K_{act}) and inactive (K_{inact}) receptor-state affinity constants, 2) the isomerization constant of the unoccupied receptor ($K_{q\text{-}obs}$), and 3) the sensitivity constant of the signaling pathway ($K_{E\text{-}obs}$). The latter two parameters define the output response of the receptor, and hence, their ratio ($K_{q\text{-}obs}/K_E$) is a useful measure of system bias. If the cellular system is reasonably stable and the $K_{q\text{-}obs}$ and $K_{E\text{-}obs}$ values of the signaling pathway are known, the K_{act} and K_{inact} values of additional agonists can be estimated in subsequent experiments on cells expressing the wild type receptor. We validated our method through computer simulation, an analytical proof, and analysis of previously published data. Our approach provides 1) a more meaningful analysis of structure-activity relationships, 2) a means of validating in silico docking experiments on active and inactive receptor structures and 3) an absolute, in contrast to relative, measure of agonist bias.

Keywords

Receptor state affinity constants; Constitutive activity; Agonist bias; System bias; Monod-Wyman-Changeux model; Observed affinity; Efficacy; Receptor activation; Active state; Inactive state

[*]Corresponding author at: Department of Pharmacology, School of Medicine, University of California, Irvine, Irvine, CA 92697-4625, United States. fjehlert@uci.edu (F.J. Ehlert).

Authorship contributions

Participated in research design: Ehlert and Stein.
Conducted Experiments: Ehlert and Stein.
Contributed to new reagents or analytic tools: Ehlert.
Performed Data Analysis: Ehlert and Stein.
Wrote or contributed to the writing of the manuscript: Ehlert and Stein.

1. Introduction

The high-resolution crystal structures of the β_2-adrenergic receptor in a complex with inverse agonist and with both agonist and G_s provide some of the most striking evidence for functional states of a G protein-coupled receptor (GPCR) (Rasmussen et al., 2007, 2011). These advances raise the question of how can the functional responses of GPCRs be analyzed to determine the affinity of drugs for receptor states?

The conventional approach for quantifying drug-receptor interactions involves measuring the parameters, observed affinity and relative efficacy. Efficacy (ε) represents the fraction of the population of ligand-receptor complexes in the active state, and the observed affinity constant, K_{obs}, the reciprocal of the concentration of ligand required for half-maximal occupancy of the receptor population (Furchgott, 1966; Furchgott & Bursztyn, 1967). For agonists, K_{obs} represents a weighted average value of the active and inactive receptor-state affinities (K_{act} and K_{inact}) (Monod, Wyman, & Changeux, 1965; Staus et al., 2016), and hence, it does not represent a measure of affinity for either state.

The relationships between affinity and efficacy and the underlying state parameters demonstrate that the product of the efficacy and observed affinity of an agonist (εK_{obs}) is proportional to the active state affinity constant (K_{act}) (Ehlert, 2015; Tran, Chang, Matsui, & Ehlert, 2009). Hence, if the εK_{obs} product of one agonist is divided by that of another, a relative estimate of K_{act} is obtained. This value was initially termed *relative intrinsic activity* (RA_i) (Ehlert, Griffin, Sawyer, & Bailon, 1999). Both null ($RA_i = \varepsilon K_{obs}/\varepsilon' K_{obs}'$) and operational ($RA_i = \tau K_{obs}/\tau' K_{obs}'$) methods of regression analysis have been developed to estimate RA_i from agonist concentration-response curves (Ehlert, 2008; Ehlert et al., 1999; Figueroa, Griffin, & Ehlert, 2008; Griffin, Figueroa, Liller, & Ehlert, 2007).

Because biased signaling involves the induction of a unique active receptor state, the RA_i value is useful for detecting agonist bias (Ehlert, 2008; Kenakin, Watson, Muniz-Medina, Christopoulos, & Novick, 2012; Tran et al., 2009). Its relative nature raises ambiguity as to which agonist is biased—the agonist of interest or the reference agonist to which the RA_i value is normalized. Ideally, the RA_i value of a test agonist is normalized relative to an agonist (e.g., natural ligand) that lacks selectivity, so that any difference in pathway RA_i values can be attributed to bias of the test agonist. Nonetheless, methods for estimating K_{act} and K_{inact} in units of M^{-1} would provide a better approach for quantifying agonist action, particularly in cases where a receptor has more than one natural ligand.

To extract these estimates from the functional responses of agonists, two problems need to be solved. First, the response to an agonist is usually measured at a point downstream in the signaling pathway, and hence, the relationship between receptor activation and response is undefined. This transducer function can be deduced (operational model, (Black & Leff, 1983; Black, Leff, Shankley, &Wood, 1985)) or eliminated from the analysis (null method, (Furchgott, 1966; Furchgott & Bursztyn, 1967)) by measuring agonist responses in the absence and presence of either partial receptor inactivation or reduced receptor expression.

The second problem is that to estimate receptor-state constants, the effect of perturbing the equilibrium between active and inactive states on the output response needs to be measured.

We recently described a protocol for estimating K_{act} and K_{inact} that relied on an allosteric agonist to push the equilibrium in the direction of the active state (Ehlert & Griffin, 2014). The approach involves measuring agonist responses under conditions of allosteric agonism and in the presence of partial receptor inactivation or reduced receptor expression. A related approach has been described for ligand-gated ion channels based on an analysis of agonist-induced whole-cell current responses (Chang & Weiss, 1999).

The equilibrium between active and inactive states can also be altered to favor the active state by introducing a constitutively activating point mutation into a GPCR. This approach has also been used to estimate the K_{act} and K_{inact} values of agonists for ligand-gated ion channels (Auerbach, 2010; Jha & Auerbach, 2010).

In this report, we describe a protocol for estimating the K_{act} and K_{inact} values of orthosteric ligands from the functional responses of GPCRs heterologously expressed in cell lines. Our method involves measuring responses of a given GPCR and a constitutively active mutant of it. Agonist responses are measured in the absence and presence of either partial receptor inactivation or reduced receptor expression. Once this analysis has been completed for one agonist, the K_{act} and K_{inact} values of additional agonists can be estimated from their concentration-response curves measured using the wild type receptor. We validate our method analytically and with simulated data and apply our approach to the analysis of published data. We also describe an example of a scenario in drug discovery to illustrate how our approach can be used to discover biased agonists (see Discussion). Our method provides a powerful means of quantifying agonist bias, investigating structure-activity relationships, and validating in silico docking experiments on active and inactive receptor structures.

2. Methods

2.1. Simulation of agonist concentration-response curves

To validate and describe our method, we simulated agonist concentration-response curves and then analyzed the data to determine if we could estimate the receptor-state constants used to simulate the data. The simulations and analyses were done using Eqs. (4)–(6), and their derivation is described next.

We have previously shown that, with regard to G protein signaling, agonist-induced receptor activation is proportional to the formation of a quaternary complex consisting of the active state of the agonist-receptor complex (*DR**) associated with exchange state of the G protein (*G**) bound with GDP (*DR*G*GDP*) (Ehlert, 2008; Ehlert & Griffin, 2014; Stein & Ehlert, 2015). We have also shown that the function describing agonist-induced formation of this complex is consistent with a Monod-Wyman-Changeux model (Ehlert & Griffin, 2014). Hence, we used the following simplified form of the Monod-Wyman-Changeux model (one orthosteric binding site and no allosteric site; (Monod et al., 1965)) to simulate agonist-receptor activation:

$$T_f = \frac{1}{1 + \frac{\mathrm{DK_{inact}} + 1}{K_{q-\mathrm{obs}}(\mathrm{DK_{act}} + 1)}} \quad (1)$$

In this equation, T_f represents the total fractional stimulus (constitutive and ligand-induced receptor activation), D, the orthosteric ligand concentration, $K_{q\text{-}obs}$, the observed isomerization constant of the unoccupied receptor, and K_{act} and K_{inact}, the active and inactive receptor-state affinity constants (units of M^{-1}). The isomerization constant ($K_q = R^*/R$) is a property of the free receptor and defines the spontaneous isomerization of the unoccupied receptor into the active state in the absence of ligands or any allosteric modulators (e.g., G proteins), whereas the observed isomerization constant ($K_{q\text{-}obs}$) describes the equilibrium between the active and inactive states of the unoccupied receptor in the presence of G protein and guanine nucleotides (Ehlert & Griffin, 2014).

To simulate a response downstream from receptor activation, we substituted Eq. (1) into the transducer function of the operational model (Black & Leff, 1983; Black et al., 1985),

$$\text{response} = \frac{M_{\text{sys}}}{1 + \left(\frac{K_{E-\text{obs}}}{T_f}\right)^m} \quad (2)$$

to yield an equation for the response to the agonist (Ehlert & Griffin, 2014):

$$\text{response} = \frac{M_{\text{sys}}}{1 + K_{E-\text{obs}}^m \left(1 + \frac{\text{DK}_{\text{inact}} + 1}{K_{q-\text{obs}}(\text{DK}_{\text{act}} + 1)}\right)^m} \quad (3)$$

In these equations, M_{sys} represents the maximum response of the signaling pathway for an agonist with infinite selectivity for the active state, m, the transducer slope factor, and $K_{E\text{-}obs}$, the observed sensitivity constant of the signaling pathway.

As described under “Results”, our protocol involves measuring the responses of both wild type and constitutively active mutant receptors under control conditions and those of reduced receptor expression or partial inactivation. Thus, Eq. (3) can be modified to account for these additional variables (Ehlert & Griffin, 2014):

$$\text{response} = \frac{M_{\text{sys}}}{1 + \left(\frac{K_{E-\text{obs}}}{\text{qB}_{\text{max-rel}}}\right)^m \left(1 + \frac{\text{DK}_{\text{inact}} + 1}{C_M K_{q-\text{obs}}(\text{DK}_{\text{act}} + 1)}\right)^m} \quad (4)$$

In this equation, $B_{max\text{-}rel}$ represents the relative receptor density of the constitutively active receptor mutant, C_M, the scalar by which the isomerization constant of the mutant receptor is increased relative to that of the wild type receptor, and q, the residual fraction of the receptor population after reduced receptor expression or partial receptor inactivation with an irreversible inverse agonist. The mutant receptor must have the same K_{act} and K_{inact} values as the wild type, and a means of validating this requirement is described under “Discussion”.

If an irreversible neutral antagonist is used to reduce the amount of orthosteric ligand binding sites, the receptor population behaves as two subpopulations – one unaffected by the

irreversible ligand and the other having its orthosteric binding pocket blocked but not its constitutive activity. For this situation, the following equation applies (Ehlert & Griffin, 2014):

$$\text{response}=\frac{M_{\text{sys}}}{1+\left(\frac{K_{E-\text{obs}}}{B_{\text{max}-\text{rel}}}\right)^{m}\left(\frac{q}{1+\frac{\text{DK}_{\text{inact}}+1}{C_M K_{q-\text{obs}}(\text{DK}_{\text{act}}+1)}}+\frac{1-q}{1+\frac{1}{C_M K_{q-\text{obs}}}}\right)^{-m}} \quad (5)$$

Finally, because the protocol involves measuring responses elicited in two populations of cells expressing either wild type or mutant receptors, an estimate of the level of receptor expression in the two cell populations is needed. The amount of receptor expression on the surface of intact cells can be estimated using a suitable radioligand. Consequently, we simulated specific binding data using the following equation:

$$B_{\text{spec}}=\frac{\text{LB}_{\text{max}-\text{rel}}B_{\text{max}-\text{WT}}}{L+K_D} \quad (6)$$

In this equation, L denotes the concentration of radioligand, K_{D}, the dissociation constant of the radioligand, $B_{max\text{-}WT}$, the binding capacity of the wild type receptor and $B_{max\text{-}rel}$, the binding capacity of the receptor population (wild type or constitutively active mutant) expressed relative to that of wild type.

The various parameters used in our nonlinear regression analysis and their definitions are listed in Table 1.

Eqs. (4) and (5) were used to simulate agonist concentration-response curves, whereas Eq. (6) was used to simulate binding data. A normally distributed random error was added to the simulated data. This was accomplished by first adding a constant background value equivalent to 0.2 M_{sys} (Eqs. (4) and (5)) or 0.2 $B_{max\text{-}WT}$ (Eq. (6)) to the simulated data. Then a 10% random Gaussian error was added (i.e., two SD resent 20%). Finally, the background value was subtracted from the data. For each analysis, we usually simulated four replicates, which are illustrated in the figures as mean ± SEM.

2.2. Nonlinear regression analysis

We analyzed the simulated functional responses and binding data using global nonlinear regression analysis with Eqs. (4)–(6) as described under Results. For this analysis, some of the parameters (K_{act}, K_{inact}, $K_{q\text{-}obs}$, $K_{E\text{-}obs}$ and K_{D}) were expressed in logarithmic form (e.g., $K_{act} = 10^{\log \text{Kact}}$). Each analysis was done on four simulated replicates of data. The theoretical curves in the figures represent the least-squares fit to all of the data, although the figures usually only show the mean data ± SEM. To estimate the SEM values of log K_{act}, log K_{inact} and other parameters, each replicate of simulated data was analyzed, and the mean ± SEM value was calculated for each parameter. We used both Prism (GraphPad Software) (Figs. 1–3, 9) and the solver function in Excel (Microsoft) (Figs. 4–8) for nonlinear regression analysis. The initial parameter estimates can be calculated from the empirical

parameters of the agonist concentration-response curves (E_{max}, EC_{50} and the constitutive response in the absence of agonist) using equations derived in Appendix A (Eqs. (19)–(29), (36), (37), (44)–(48), (54)). A detailed description of our methods of analysis is given in the online Supplement.

2.3. Monte Carlo analysis

We performed a Monte Carlo analysis of our regression technique (Eq. (4)) to examine how the distribution of parameter estimates for a single agonist is related to random error in the simulated data. This was accomplished using a script that took advantage of the automated simulation and nonlinear analysis functions of the Prism application (Fig. 2). For analyses involving more than one agonist with Eq. (4) or analyses with Eq. (5) (Figs. 5, 7 and 8), we manually performed simulations using Excel.

2.4. Analysis of published data

To illustrate the feasibility of our analysis technique we applied it to published agonist concentration-response curves of muscarinic agonist-induced responses on wild type and constitutively active mutant receptors. This was accomplished using the GraphClick application (Arizona Software) to estimate response values from electronic images of published data. The data were subsequently analyzed by global nonlinear regression analysis as described under “Results”.

3. Results

3.1. Analysis of simulated data, full agonist

The concentration-response curves of an agonist for eliciting a response through a wild type and constitutively active mutant receptor were simulated using Eq. (4), and the results are shown in Fig. 1. Data were simulated for the conditions of control and reduced receptor expression or partial receptor inactivation with an irreversible inverse agonist (panel *a*). The simulations were for a highly efficacious agonist having 10^4-fold higher affinity for the active state (log K_{act}, 8.0) relative to the inactive state (log K_{inact}, 4.0). The isomerization constant of the unoccupied wild type receptor was 10^{-4} (log $K_{q\text{-}obs}$, −4), whereas that of the constitutively active mutant was approximately fiftyfold greater (log C_M, 1.7). We also simulated binding data using Eq. (6) to represent the results of saturation binding experiments on the cells expressing wild type and mutant receptors (panel *b*). The plots in Fig. 1 show the mean ± SEM values of four simulations.

The data for each simulation were analyzed by global nonlinear regression analysis using Eqs. (4) and (6), and the mean parameter estimates ± SEM values are listed in Table 2. During the analysis, the estimates of M_{sys}, m, log K_{act}, log K_{inact}, log $K_{q\text{-}obs}$ and log $K_{E\text{-}obs}$ were shared among the four concentration-response curves. The value of parameter $B_{max\text{-}rel}$ was constrained to 1.0 for the wild type receptor binding and functional data, and a shared value was estimated by regression analysis of the mutant receptor binding and functional data. A shared estimate of $B_{max\text{-}WT}$ was obtained from the simulated binding data. Finally, individual estimates of the fraction of the residual receptor population after reduced expression or partial receptor inactivation (q) were obtained for the appropriate wild type

and mutant receptor functional data. This latter parameter was constrained to 1.0 for the functional data lacking a depleted receptor population (control).

Table 2 lists the parameter estimates from regression analysis as well as the parameter values used to simulate the data. As shown in the table, accurate estimates with reasonable SEM values could be obtained for all of the parameters with four replicates, including the receptor-state parameters (log K_{act}, K_{inact} and $K_{q\text{-}obs}$). The parameters with the largest relative variance included the isomerization constant of the unoccupied receptor (log $K_{q\text{-}obs}$, SD, 0.13) and the inactive receptor-state affinity constant (log K_{inact}, SD, 0.26).

To determine the variation in parameter estimates more accurately, we simulated 1020 experiments, each with a sample size of 4, and analyzed these by global nonlinear regression analysis. The mean parameter estimates ± standard deviation were: log K_{act}, 7.99 ± 0.10; log K_{inact}, 3.95 ± 0.22; log $K_{q\text{-}obs}$, −3.98 ± 0.26; log $K_{E\text{-}obs}$, −1.99 ± 0.15; log C_M, 1.70 ± 0.085; q_{WT}, 0.021 ± 0.004; q_M, *0.021* ± 0.006; M_{sys}, 1.00 ± 0.022; m, 1.52 ± 0.17; log $K_{\text{D-}WT}$, −10.00 ± 0.043; $B_{max\text{-}WT}$, 1.00 ± 0.034 and $B_{max\text{-}rel}$, 0.80 ± 0.032. Note that these standard deviations represent the variation in a parameter estimated from a sample size of four. Hence, they represent an average estimate of the expected SEM value for a sample size of four. Notwithstanding the small sample size, the SEM values in Table 2 are generally consistent with this prediction. The distributions (probability density functions) of the parameter estimates, K_{act}, K_{inact}, $K_{q\text{-}obs}$ and $K_{E\text{-}obs}$, are shown in Fig. 2.

In 1.3% of the cases, however, it was impossible to obtain an accurate estimate of log K_{inact} even though reliable estimates of the other parameters were obtained. To investigate this phenomenon, we analyzed individual simulations (i.e., N = 1) to determine how the residual sum of squared deviations of the data points from the regression equation (*RSS*) is affected by constraining the value of log K_{inact} to various values near the best fitting estimate. Fig. 3*a* shows an example of a simulation from which a reasonable estimate of log K_{inact} was obtained (log K_{inact}, 3.97; theoretical value, 4.0). The upper panel in Fig. 3*d* shows how RSS changes as the least-squares regression is done with K_{inact} constrained to various values indicated on the abscissa. The plot shows that RSS is at a minimum when log K_{inact} = 4.0. An increase in RSS occurs whenever log K_{inact} is constrained to values larger or smaller than the best fitting estimate although the increase in RSS is not much when K_{inact} < 4.0. The lower panel in Fig. 3*d* shows how the estimates of selected parameters change when the regression is done with K_{inact} constrained to various values. Small changes in these parameter estimates occur when the K_{inact} is constrained to values < 4.0 during the regression.

In contrast, Fig. 3*b* shows an example of a simulation for which a reliable estimate of log K_{inact} was impossible. In this case, RSS is at a constant minimum value whenever log K_{inact} is constrained to a value less than approximately 3.0 (upper panel, Fig. 3*e*). Over this range, the estimates of log K_{act}, log K_q and log K_E are nearly constant at values (7.68, −3.52 and −1.83, respectively) that are reasonable (theoretical values, 8.0, −4.0 and −2.0) given the large error in the data (lower panel, Fig. 3*e*). Not surprisingly, we found that reducing the size of the random error or increasing the sample size or the number of agonist

concentrations in the simulation reduced the likelihood of obtaining a simulated data set for which K_{inact} was inestimable.

Finally, Fig. 3*c* shows an example of data with no error. When regression analysis is done with log K_{inact} constrained to values greater or less than that used to simulate the data (log K_{inact}, 4.0) an increase in RSS occurs (upper panel, Fig. 3f). Thus, like the simulated data shown in Fig. 3*a* and *d*, a least-squares fit is obtained when K_{inact} is equal to or approximately equal to 4.0, and the topography of the plot of RSS against log K_{inact} shows a clear minimum. The gradient of the plot in the direction $K_{inact} < 4$ is not substantial, however.

We also simulated functional data similar to that shown in Fig. 1, but for the case involving the use of an irreversible neutral antagonist to reduce the size of the receptor population (Fig. 4*a*). The mean ± SEM of four simulations are shown. These data together with the receptor binding data in Fig. 4*b* were analyzed simultaneously by global nonlinear regression analysis with Eqs. (5) and (6). The parameter estimates were shared as described above in connection with the simulated data in Fig. 1. Regression analysis yielded parameter estimates with reasonable SEM values that were nearly the same as the parameters used to simulate the data. Parameter estimates for this simulation are included in Table 2.

To investigate the variation in parameter estimates for the simulation shown in Fig. 4, we carried out 150 Monte Carlo simulations manually using Excel. Each simulation consisted of four replicates. The resulting probability density functions for log K_{inact}, log K_{act}, log $K_{q\text{-}obs}$ and log $K_{E\text{-}obs}$ are shown in Fig. 5. Out of 150 simulations, there was only one case where it was impossible to estimate log K_{inact}. The average parameter estimates and their standard deviations for the 149 cases in which all of the parameters were estimable were: log K_{act}, 8.01 ± 0.13; log K_{inact}, 3.96 ± 0.29; log $K_{q\text{-}obs}$, −4.05 ± 0.28; log $K_{E\text{-}obs}$, −2.03 ± 0.15; log C_M, 1.71± 0.11; q_{WT}, 0.021 ± 0.005; q_M, 0.020 ± 0.0046; M_{sys}, 1.00 ± 0.021; m, 1.49 ± 0.22; log $K_{\text{D-}WT}$, −9.99 ± 0.051; $B_{max\text{-}WT}$, 1.01±0.034 and $B_{max\text{-}rel}$, 0.80 ± 0.043. The standard deviations represent the expected SEM value for a sample size of four and are similar to the corresponding values given in Table 2 for the simulation shown in Fig. 4.

3.2. Analysis of a group of agonists

Once the large data set shown for the full agonist in Figs. 1 or 4 is obtained, all that is required to estimate the receptor-state constants of additional agonists are their concentration-response curves measured in experiments on the wild type receptor. For full agonists, experiments in the presence of partial receptor inactivation or reduced receptor expression are also needed.

Fig. 6 shows mean values ± SEM (N = 4) of simulated functional data for a full agonist (test agonist 1) and three partial agonists (test agonists 2–4). These data were analyzed simultaneously with those shown in Fig. 1 (reference agonist), and the resulting parameter estimates from global nonlinear regression analysis are listed in Table 3. These estimates were similar to the values used in the simulation, which are also listed in Table 3.

To examine the distribution and variance of parameter estimates we carried out 128 simulations manually using Excel and estimated the standard deviations of the parameter estimates obtained from samples consisting of four replicates. In one of these simulations, it was impossible to obtain an estimate of log K_{inact} for the reference agonist. For the remaining 127 simulations, the mean ± SD of the parameters for the reference agonist are: log K_{act}, 8.00 ± 0.090 and log K_{inact}, 3.99 ± 0.18. The parameters of the test agonists are: test agonist 1: log K_{act}, 7.50 ± 0.10 and log K_{inact}, 4.00 ± 0.11; test agonist 2; log K_{act}, 6.50 ± 0.10 and log K_{inact}, 4.00 ± 0.12; test agonist 3: log K_{act}, 6.00 ± 0.11 and log K_{inact}, 4.00 ± 0.075; test agonist 4, log K_{act}, 5.51 ± 0.14 and log K_{inact}, 4.01 ± 0.12. Finally, the parameters of the receptor and signaling pathway are: M_{sys}, 1.00 ± 0.018, m, 1.51 ± 0.11; log $K_{q\text{-}obs}$, −4.01 ± 0.21, log $K_{E\text{-}obs}$, −2.00 ± 0.12; log C_M, 1.70 ± 0.078; q_{WT}, 0.021 ± 0.0033; q_{Mut}, 0.020 ± 0.0046. These mean estimates are nearly the same as the values used to simulate the data (see Table 3). The standard deviations of the parameters of the test agonists are comparable to the SEM values of the corresponding parameter estimates in Table 3, which were calculated from a sample size of four.

The probability density functions for the log K_{act} values of the agonists are shown in Fig. 7. The values for log K_{act} used to generate the simulations were 7.5, 6.5, 6.0 and 5.5, for test agonists 1–4, respectively. The corresponding distributions for the estimates of log K_{inact} are shown in Fig. 8. The value of log K_{inact} used to generate the simulations was 4.0 for all of the agonists.

The data for the test agonists can also be analyzed simultaneously with the data in Fig. 4 for those situations in which an irreversible neutral antagonist is used to deplete the receptor populations. When this analysis was done, results similar to those described above were obtained (Table 3).

3.3. Analysis of data from the literature

Spalding, Burstein, Wells, and Brann (1997) investigated how a series of constitutively activating point mutations affected the concentration-response curves of carbachol for stimulating growth in HEK cells transiently expressing the M_5 muscarinic receptor. We analyzed data presented in Fig. 7 of their manuscript to determine how accurately we could estimate the K_{act} and K_{inact} values of carbachol. These data are illustrated in Fig. 9*a* of the present manuscript. Shown are the mean response values for carbachol-stimulated growth by the wild type M_5 receptor and six point mutants of serine 465 (glycine, proline, tryptophan, valine, arginine and lysine). Spalding et al. (1997) showed that there were no significant differences in the expression of wild type and mutant receptors. Hence, Eq. (4) was used in the analysis with the parameter $B_{max\text{-}rel}$ constrained to 1.0 for all data sets. Regression analysis of the mean data yielded parameter estimates ± asymptotic SE values of log K_{inact}, 5.48 ± 0.13; log K_{act}, 8.54 ± 0.11; M_{sys}, 218 ±29; and m, 0.55 ± 0.048. The log values for the scalar increases in $K_{q\text{-}obs}$ (log C_M) caused by the S465G, S465P, S465W, S465V, S465R and S465K point mutations were 0.49 ± 0.075; 0.73 ± 0.085, 1.25 ± 0.11, 2.11 ± 0.14, 2.41 ± 0.15 and 2.90 ± 0.19, respectively. It was impossible to obtain accurate estimates of log $K_{q\text{-}obs}$, and log $K_{E\text{-}obs}$.

To determine the variability in parameter estimates from data like those shown in Fig. 9*a*, we simulated analogous data using Eq. (4), with the parameters q and $B_{max\text{-}rel}$ assigned values of 1.0. The mean simulated response values of four replicates ± SEM are shown in Fig. 9*b*. We also carried out 151 simulations using Excel, with each simulation having four replicates. The mean parameters estimates ± SD for these simulations (K_{inact}, 4.00 ± 0.094; K_{act}, 6.99 ± 0.089; M_{sys}, 1.04 ± 0.13; and m, 1.57 ± 0.15) were similar to values used to generate the data (4.0, 7.0, 1.0 and 1.5, respectively). The log values for the scalar increases in $K_{q\text{-}obs}$ (log C_M) caused by the CAM 1–5 mutations (0.60 ± 0.062; 1.20 ± 0.082, 1.80 ± 0.085, 2.39 ± 0.10 and 2.90 ± 0.19) were also similar to those used to simulate the data (0.6, 1.2, 1.8, 2.4 and 3.0, respectively). Again these SD values represent the average SEM value expected for a sample size of four. Although it was possible to estimate the composite parameter, log $K_{q\text{-}obs}/[(1 + K_{q\text{-}obs})K_{E\text{-}obs}]$, accurately (−2.98 ± 0.16; value used in simulation, −2.803), mean estimates of the individual parameters, $K_{q\text{-}obs}$ and $K_{E\text{-}obs}$, were off by about one log unit and had SD values >1.6 log units. At the population level of analysis, the latter composite parameter is equivalent to the τ value for the unoccupied receptor (i.e., constitutive activity, τ_{sys}) (Ehlert, Suga, & Griffin, 2011).

4. Discussion

To apply our analysis, a constitutively active receptor mutant is needed that has K_{act} and K_{inact} values for ligands that are the same as those of the wild type receptor. Given our present state of knowledge of GPCR structure and activation (Manglik et al., 2015; Nygaard et al., 2013), it should be possible to identify residues sufficiently far from the orthosteric binding pocket that cause constitutive receptor activation when mutated. One approach for identifying an appropriate receptor mutant is to first analyze a number of potential mutants. If each mutant yields the same estimates of K_{act} and K_{inact} for a given agonist, then it would seem that the mutations only alter the isomerization constant ($K_{q\text{-}obs}$) without affecting ligand affinity for receptor states.

Two examples of such an analysis are illustrated in Fig. 9, which shows simulated data (panel *b*) and the experiments of Spalding et al. (1997) (panel *a*). The global regression analysis is based on the assumption that the values of K_{act} and K_{inact} for the wild type and mutant receptors are the same and that the mutations only affect $K_{q\text{-}obs}$. This mutation-induced increase in $K_{q\text{-}obs}$ causes predictable increases in agonist potency and the basal response in the absence of agonist. If there were changes in K_{act} and K_{inact}, then the best fitting curves would not align with the data points because changes in K_{act} and K_{inact} affect EC_{50} beyond that caused by changes in $K_{q\text{-}obs}$. The good agreement between the data points and the global best fitting curve shows that the mutations only affected $K_{q\text{-}obs}$ and not K_{act} and K_{inact}. Hence, any one of the mutants that caused a measureable constitutive response (e.g., >10% E_{max}) would be useful for our analysis.

The forgoing results are consistent with the premise that ligands select for pre-existing states of the receptor depending on their differential affinity for each state (Monod-Wyman-Changeux model; (Monod et al., 1965)). Agonists exhibit high affinity for the active state relative to the inactive, and consequently, shift the equilibrium in the direction of the active state. This change is accomplished by an agonist-induced increase in the isomerization

constant of the unoccupied receptor ($[R]/[R^*] = K_{q\text{-}obs}$) by the factor, K_{act}/K_{inact} (i.e., $[DR^*]/[DR] = K_{qobs}K_{act}/K_{inact}$). This mechanism implies that a constitutively activating point mutation should increase the observed affinity of an agonist (K_{obs}) by increasing the isomerization constant and not by altering the affinity of the agonist for active and inactive receptor states. The results in Fig. 9 are consistent with this postulate.

The response shown in Fig. 9*a* involves agonist-induced proliferation of new receptor-expressing cells. The total receptor population increases in time and reaches a plateau as the response (proliferation) desensitizes throughout the lengthy five-day incubation with agonist. Though not often appreciated, these dynamics can be analyzed accurately using the reverse engineering approach inherent in the transducer function of the operational model. To validate this hypothesis, we used Gompertzian kinetics to simulate an agonist-induced exponential increase in cellular proliferation that slows down with time. We substituted this receptor activation function into the transducer function of the operational model and simulated data with a 10% Gaussian error. These data were analyzed by global nonlinear regression analysis with Eq. (4) (see Supplemental data). We were able to accurately estimate the log K_{act} and K_{inact} values used to simulate the data.

NMR studies of purified β_2-adrenergic (Manglik et al., 2015; Nygaard et al., 2013) and A_{2A} adenosine (Ye, Van Eps, Zimmer, Ernst, & Prosser, 2016) receptors reveal that the unoccupied receptor undergoes transitions between two inactive states. Similarly, the agonist-occupied receptor also interconverts between a transition state and a fully active state. Full activation of the β_2-adrenergic receptor requires G_s or a G protein mimetic nanobody. The loci of conformational flexibility are the cytosolic ends of helices that interact with G protein (TM3, 5 and 6). These results imply that in the absence of G protein the binding pocket structures of the active and inactive states of the receptor are associated with more flexible conformations of the cytosolic ends of helices 3, 5 and 6 (Manglik et al., 2015; Nygaard et al., 2013). These NMR studies are also consistent with the postulate that ligand binding mainly causes a change in the relative abundances of pre-existing receptor states and not the generation of new states.

Recent studies illustrate how stabilizing the β_2-adrenergic receptor in the active or inactive state with nanobodies affects the binding of various ligands to the receptor (Staus et al., 2016). The total change in the affinity of isoproterenol that occurred when the receptor was stabilized in the active state relative to inactive was 15,000-fold. Again these results are consistent with the consequences of the Monod Wyman Changeux model, although more than two states were needed to describe the data for all of the agonists investigated in this study.

For our pharmacological analysis, receptor states are defined in terms of their affinity for ligands (K_{act} and K_{inact}) and their corresponding ability to generate a response (active and inactive). This provision implies specific structural features of the ligand-binding pocket that are linked to complementary features of the cytosolic ends of the helices that interact with G protein. That is, the active state of the receptor has high affinity for its natural agonist ligand and the distal ends of helices 3, 5 and 6 form stable interactions with the guanine nucleotide-free form of the holo G protein. In the inactive state, the receptor has low affinity for its

natural agonist, and the cytosolic ends of its helices are flexible as they catch GDP bound G proteins or perhaps are somewhat more stabilized when the latter are present. Of course, biased agonists may induce or stabilize unique active states that bias signaling.

If there is conformational variability in the binding pockets of the active and inactive states then our analysis would yield weighted ensemble average affinity estimates for the active (log K_{act}) and inactive (log K_{inact}) states.

We used simulation to validate our analysis and to show how to apply it to the analysis of data. A more direct way to achieve the former goal is to demonstrate that the receptor-state constants can be calculated from the empirical parameters of the concentration-response curves (EC_{50}, E_{max} and constitutive response) of our assay protocol. In the Appendix A, we derive equations that express the EC_{50}, E_{max} and constitutive response values in terms of the state parameters of Eqs. (4) and (5) for the case of a transducer slope factor of one ($m = 1$). We solved these equations for the receptor-state constants and verified that state parameters could be estimated from the EC_{50}, E_{max} and constitutive response values of simulated data with substantial random error. These equations can also be used to generate initial parameter estimates for regression analysis of data having Hill slopes differing from one, such as those presented under “Results”. In a prior analysis, we published a set of equations that can be used to derive receptor-state and population constants from the graphical parameters of the concentration-response curves measured in experiments investigating allosteric interactions (Ehlert & Griffin, 2014).

Our approach can also be applied to data sets lacking the full complement of concentration-response curves shown in Figs. 1*a* and 4*a*. If either one or both curves for the condition of a reduced receptor population are lacking, it may be impossible to estimate some or all of the three parameters, K_{inact}, $K_{q\text{-}obs}$ or $K_{E\text{-}obs}$, depending on whether a full or partial agonist is investigated (see Table 4).

Our experimental protocol and analysis involving wild type and mutant receptors (see Figs. 1 and 4) provides estimates of two parameters ($K_{E\text{-}obs}$ and $K_{q\text{-}obs}$) that define the properties of the signaling pathway for a given output response. Hence, once the initial characterization is completed for a given full agonist, the receptor-state constants of additional agonists can be estimated using the cells expressing the wild type receptor provided that the signaling properties of the latter are reasonably stable. An analogous approach employing an allosteric agonist to increase constitutive receptor activity could be used to estimate the $K_{E\text{-}obs}$ and $K_{q\text{-}obs}$ values of specific output responses in native cells and tissues (Ehlert & Griffin, 2014), which typically exhibit invariant EC_{50} and E_{max} values for a given response over time. Having accurate values of $K_{E\text{-}obs}$ and $K_{q\text{-}obs}$ would enable investigators to estimate the receptor-state constants of additional ligands from an analysis of their concentration-response curves in native preparations including those previously published.

As mentioned, the parameters $K_{E\text{-}obs}$ and $K_{q\text{-}obs}$ define the sensitivity of the output response. Sensitivity increases with a decrease in $K_{E\text{-}obs}$ and an increase in $K_{q\text{-}obs}$. Hence, a useful measure of the sensitivity of the output response of a given signaling pathway is the ratio, $K_{q\text{-}obs}/K_{E\text{-}obs}$. Since $K_{q\text{-}obs}$ is a small number ($K_{q\text{-}obs} < 1$), a nearly equivalent expression is,

$K_{q\text{-}obs}/((1 + K_{q\text{-}obs})K_{E\text{-}obs})$. This latter expression is equivalent to the population parameter, τ_{sys}, which is a measure of constitutive activity (Ehlert, Suga, et al., 2011). Thus, the system bias of one pathway ($\tau_{sys\text{-}1}$) relative to another ($\tau_{sys\text{-}2}$) can be expressed as $\tau_{sys\text{-}1}/\tau_{sys\text{-}2}$ or $\log \tau_{sys\text{-}1}/\tau_{sys\text{-}2}$ ($\log \Delta\tau_{sys}$). Alternatively, the ratio of the $K_{q\text{-}obs}/K_{E\text{-}obs}$ value of each pathway can be used to estimate system bias.

An advantage of estimating agonist K_{act} and K_{inact} values is that, for a given signaling pathway, these estimates do not change with variation in the expression of G proteins or the concentration of GTP (Ehlert, Griffin, & Suga, 2011). The latter allosteric modulators have effects that are indistinguishable from a change in the isomerization constant ($K_{q\text{-}obs}$). As shown from the analysis associated with Fig. 9, such a change does not influence the estimates of K_{act} and K_{inact}. Similarly, numerous receptor associated proteins have been described that influence receptor expression and the sensitivity of signaling pathways (Bruneau, Esteban, & Akaaboune, 2009; Guo, Sun, Hamet, & Inagami, 2001; Ruiz de Azua et al., 2012). Such proteins would be expected to alter the sensitivity constant of the signaling pathway ($K_{E\text{-}obs}$) but not K_{act} and K_{inact}.

Whenever a ligand induces a conformational change in a receptor, the population parameter of observed affinity (reciprocal of the observed dissociation constant; i.e., $K_{obs} = 1/K_D$) does not reflect agonist affinity for any stable receptor structure (Jencks, 1975; Monod et al., 1965). Rather, observed affinity, or K_D ($1/K_{obs}$), determines receptor occupancy of both active and inactive receptor states (occupancy = $X/(X + K_D)$, where X denotes the agonist concentration). Hence, receptor-state affinity constants are essential in understanding how drugs bind to receptor structures, particularly when drugs are docked onto active and inactive receptor structures, in silico. Consequently, the K_{act} and K_{inact} values of ligands provide more meaningful information in structure-activity relationships than estimates of EC_{50}, E_{max}, K_{obs} and ε. It is, nonetheless, always possible to estimate the latter parameters once the receptor-state parameters are known (see Ehlert and Griffin (2014)).

Receptor-state affinity constants are useful for quantifying agonist bias because the associated mechanism involves agonist induction of a unique-active receptor state that selectively engages the transducer protein of one pathway (e.g., G_i) relative to that of another (e.g., GRK). To mediate this selective transduction, the agonist must have higher affinity for the receptor state that couples to G_i relative to that which interacts with GRK and recruits β-arrestin, or alternatively, the agonist induces a unique state that activates G_i but does not recruit GRK or β-arrestin effectively. Either mechanism would yield a difference in the estimates of K_{act} for the two responses. Thus, our approach provides a quantitative measure for calculating agonist bias.

For example, consider the hypothetical case of screening for agonists of the GPR109A receptor. Such agents are potentially useful in the treatment of dyslipidemias, but the receptor also mediates the unwanted side effect of cutaneous flushing (Guyton, 2004, 2007). This latter effect is contingent upon activation of both G protein ($G_{i/o}$) and β-arrestin signaling, whereas the beneficial responses of reducing triglycerides and increasing HDL levels are mediated through $G_{i/o}$ signaling only (Richman et al., 2007; Walters et al., 2009).

Hence, a GRP109A agonist with a bias for G protein over β-arrestin signaling should be a useful therapeutic agent for treating dyslipidemias (Whalen, Rajagopal, & Lefkowitz, 2011).

To screen for such an agent, agonist-induced inhibition of cAMP accumulation ($G_{i/o}$ signaling) and stimulation of arrestin recruitment could be measured in HEK293 cells as described by Walters and coworkers (Walters et al., 2009). Complete concentration-response curves could be measured for a known agonist, such as nicotinic acid, under control conditions and after reduced receptor expression using both wild type and constitutively active mutant receptors. Additional potentially biased agonists could be screened on the wild type receptor only, and the data analyzed as described above in connection with Figs. 1 and 6 and Table 3.

Analysis of the in vitro screening data would yield estimates of the receptor-state affinity constants (K_{act} and K_{inact}) of the agonists. In the simplest case, the estimate of inactive-state affinity for a given agonist would be the same for both G protein and β-arrestin signaling. Under such conditions, an agonist biased for G protein signaling would have a higher active-state affinity (larger log K_{act} value) for G protein signaling relative to that measured for β-arrestin signaling. For agonists that exhibit changes in both K_{act} and K_{inact} across the two assays, a bias for G protein signaling is manifest as both a larger K_{act} value and a larger K_{act}/K_{inact} ratio. This latter ratio is equivalent to efficacy at the receptor-state level of analysis (Ehlert, 2000; Ehlert, 2015).

One could compare clinical effectiveness in vivo with the K_{act}/K_{inact} ratio estimated in vitro to glean what degree of receptor activation is useful therapeutically. Presumably, an increase in drug affinity (increase in the values of K_{act} and K_{inact}) while maintaining an ideal K_{act}/K_{inact} ratio would yield an agent with higher potency and possibly fewer off-target effects. In this way, in vitro drug discovery can be facilitated by seeking drugs with optimum K_{act} and K_{inact} values.

While our analysis would provide estimates of the system bias of each pathway in vitro (i.e., log $\Delta\tau_{sys,}$ see above), these values may not reflect the corresponding values for the responses observed in patients in vivo because of potential differences in the expression of signaling proteins (e.g., G proteins) and the concentration of GTP. In addition, the measured step in the signaling pathway in the cell lines is often more proximal to receptor activation as compared to the final clinical response in vivo. This difference will also influence system bias. Finally, differences in the expression of receptors and G proteins and the concentration of GTP in the cell line compared to the corresponding conditions in native tissues in vivo can influence the population parameters of observed affinity and efficacy. By contrast, receptor-state affinity constants are unaffected by these factors.

Methods for deriving an estimate of bias based on the differential ability of an agonist to elicit responses through the different signaling pathways of a given receptor have been reviewed (Kelly, 2013; Kenakin & Christopoulos, 2013) and described (Zhang & Kavana, 2015, 2016). Many of these protocols represent ingenious ways of analyzing the results of screening assays to deduce the efficacy of agonists at the receptor population level of analysis.

To summarize, our approach provides a means of calculating an absolute measure of 1) system bias, based on pathway sensitivity and the isomerization constant of the unoccupied receptor (τ_{sys} or ($K_{q\text{-}obs}$/((1 + $K_{q\text{-}obs}$)$K_{E\text{-}obs}$), and agonist bias, based on both 2) active state affinity (K_{act}) and 3) receptor activation (K_{act}/K_{inact}). These parameters should provide a more quantitative and standardized measure of drug action across different assays and a better means of relating activity to receptor structures and the final clinical outcome.

Supplementary Material

Refer to Web version on PubMed Central for supplementary material.

Appendix A

To prove that receptor-state constants can be estimated from the type of data analyzed in this report, we derived equations that express receptor-state parameters in terms of the graphical parameters of the agonist concentration-response curves (i.e., EC_{50}, E_{max} and constitutive response in the absence of agonist) used in our analysis for the case of a transducer slope factor equivalent to one (m = 1). Note that these equations can also be used to derive initial parameter estimates for global nonlinear regression analysis with Eqs. (4) and (5) regardless of the value of the transducer slope factor.

The variables representing the graphical parameters are defined in Fig. 10 for cases involving reduced receptor expression or partial receptor inactivation with an irreversible inverse agonist (panel *a*) or an irreversible neutral antagonist (panel *b*). First, we derive equations for the graphical parameters, expressed in terms of receptor-state constants. Then we solve these equations to express receptor-state constants in terms of graphical parameters.

A.1. Reduced receptor expression or partial receptor inactivation with an irreversible inverse agonist

For the case illustrated in Fig. 10*a*, there are four conditions, 1) wild type, control; 2) wild type, reduced expression; 3) constitutively active mutant (CAM), control; and 4) CAM, reduced expression. The graphical parameters for these conditions (E_{max}, E; basal response, B and EC_{50}, EC) are denoted with subscripts corresponding to conditions 1–4. The pharmacological responses for these four conditions are described by Eq. (4), but with constraints placed on variables q and C_M to specify each condition: condition 1, q = 1, C_M = 1; condition 2, q = Q_1, C_M = 1; condition 3, q = 1; and condition 4, q = Q_2. With these substitutions, equations for the E_{max} values (E_1–E_4) are derived by taking the limit of Eq. (4) as the agonist concentration (D) approaches infinity:

$$E_1 = \frac{M_{\text{sys}} K_{\text{act}} K_{q-\text{obs}}}{K_{\text{inact}} K_{E-\text{obs}} + K_{\text{act}} K_{q-\text{obs}} (K_{E-\text{obs}} + 1)} \quad (7)$$

$$E_2=\frac{M_{\mathrm{sys}}K_{\mathrm{act}}K_{q-\mathrm{obs}}Q_1}{K_{\mathrm{inact}}K_{E-\mathrm{obs}}+K_{\mathrm{act}}K_{q-\mathrm{obs}}(K_{E-\mathrm{obs}}+Q_1)} \quad (8)$$

$$E_3=\frac{M_{\mathrm{sys}}K_{\mathrm{act}}K_{q-\mathrm{obs}}C_M B_{\mathrm{max-rel}}}{K_{\mathrm{inact}}K_{E-\mathrm{obs}}+K_{\mathrm{act}}K_{q-\mathrm{obs}}C_M(K_{E-\mathrm{obs}}+B_{\mathrm{max-rel}})} \quad (9)$$

$$E_4=\frac{M_{\mathrm{sys}}K_{\mathrm{act}}K_{q-\mathrm{obs}}C_M Q_2 B_{\mathrm{max-rel}}}{K_{\mathrm{inact}}K_{E-\mathrm{obs}}+K_{\mathrm{act}}K_{q-\mathrm{obs}}C_M(K_{E-\mathrm{obs}}+Q_2 B_{\mathrm{max-rel}})} \quad (10)$$

In these equations, Q_1 and Q_2 denote the residual fraction of receptors after reduced receptor expression of wild type and mutant receptors, respectively, $B_{max\text{-}rel}$, the receptor density of the mutant receptor expressed relative to wild type, and C_M, the scalar increase in K_q in the constitutively active mutant receptor.

Equations for the basal response values in the absence of agonist (B_1–B_4) are derived by taking the limit of Eq. (4) as the agonist concentration (D) approaches zero:

$$B_1=\frac{M_{\mathrm{sys}}K_{q-\mathrm{obs}}}{K_{E-\mathrm{obs}}+K_{q-\mathrm{obs}}(K_{E-\mathrm{obs}}+1)} \quad (11)$$

$$B_2=\frac{M_{\mathrm{sys}}K_{q-\mathrm{obs}}Q_1}{K_{E-\mathrm{obs}}+K_{q-\mathrm{obs}}(K_{E-\mathrm{obs}}+Q_1)} \quad (12)$$

$$B_3=\frac{M_{\mathrm{sys}}K_{q-\mathrm{obs}}C_M B_{\mathrm{max-rel}}}{K_{E-\mathrm{obs}}+K_{q-\mathrm{obs}}C_M(K_{E-\mathrm{obs}}+B_{\mathrm{max-rel}})} \quad (13)$$

$$B_4=\frac{M_{\mathrm{sys}}K_{q-\mathrm{obs}}C_M Q_2 B_{\mathrm{max-rel}}}{K_{E-\mathrm{obs}}+K_{q-\mathrm{obs}}C_M(K_{E-\mathrm{obs}}+Q_2 B_{\mathrm{max-rel}})} \quad (14)$$

It can be shown that when the agonist concentration is equal to EC_{50}, the response is equal to the average of the maximal and basal responses ($0.5(B_1 + E_1)$) (Ehlert, Suga, et al., 2011). This relationship can be represented by substituting EC_{50} for D in Eq. (4) and setting the resulting equation equal to the EC_{50} response defined in the prior sentence. Solving this relationship for EC_{50} yields:

$$\mathrm{EC}_1=\frac{K_{E-\mathrm{obs}}+K_{q-\mathrm{obs}}(K_{E-\mathrm{obs}}+1)}{K_{\mathrm{inact}}K_{E-\mathrm{obs}}+K_{\mathrm{act}}K_{q-\mathrm{obs}}(K_{E-\mathrm{obs}}+1)} \quad (15)$$

$$\mathrm{EC}_2=\frac{K_{E-\mathrm{obs}}+K_{q-\mathrm{obs}}(K_{E-\mathrm{obs}}+Q_1)}{K_{\mathrm{inact}}K_{E-\mathrm{obs}}+K_{\mathrm{act}}K_{q-\mathrm{obs}}(K_{E-\mathrm{obs}}+Q_1)} \quad (16)$$

$$\mathrm{EC}_3=\frac{K_{E-\mathrm{obs}}+K_{q-\mathrm{obs}}C_M(K_{E-\mathrm{obs}}+B_{\mathrm{max-rel}})}{K_{\mathrm{inact}}K_{E-\mathrm{obs}}+K_{\mathrm{act}}K_{q-\mathrm{obs}}C_M(K_{E-\mathrm{obs}}+B_{\mathrm{max-rel}})} \quad (17)$$

$$\mathrm{EC}_4=\frac{K_{E-\mathrm{obs}}+K_{q-\mathrm{obs}}C_M(K_{E-\mathrm{obs}}+Q_2B_{\mathrm{max-rel}})}{K_{\mathrm{inact}}K_{E-\mathrm{obs}}+K_{\mathrm{act}}K_{q-\mathrm{obs}}C_M(K_{E-\mathrm{obs}}+Q_2B_{\mathrm{max-rel}})} \quad (18)$$

The foregoing equations are solved to yield expressions for the various parameters of the receptor states and transducer function, expressed in terms of the graphical parameters of the concentration-response curves. We begin with the maximal response of the system (M_{sys}), which can be estimated from the graphical parameters of the wild type receptor:

$$M_{\mathrm{sys}}=\frac{E_1(E_1\mathrm{EC}_2-E_2\mathrm{EC}_1)+B_1\mathrm{EC}_1(E_2-E_1)}{E_1(\mathrm{EC}_2-\mathrm{EC}_1)} \quad (19)$$

When the constitutive response of the wild type receptor is immeasurable (B_1 = 0), Eq. (19) reduces to:

$$M_{\mathrm{sys}}=\frac{E_1\mathrm{EC}_2-E_2\mathrm{EC}_1}{\mathrm{EC}_2-\mathrm{EC}_1} \quad (20)$$

M_{sys} can also be estimated from the graphical parameters of the constitutively active mutant receptor:

$$M_{\mathrm{sys}}=\frac{E_3(E_3\mathrm{EC}_4-E_4\mathrm{EC}_3)+B_3\mathrm{EC}_3(E_4-E_3)}{E_3(\mathrm{EC}_4-\mathrm{EC}_3)} \quad (21)$$

The fraction of the residual population of wild type receptors after reduced receptor expression or partial receptor inactivation with an irreversible inverse agonist (Q_1) is given by:

$$Q_1 = \frac{E_2 \mathrm{EC}_1 (E_1 - B_1)}{E_1 (E_1 \mathrm{EC}_2 - B_1 \mathrm{EC}_1)} \quad (22)$$

When the constitutive response of the wild type receptor is immeasurable ($B_1 = 0$), Eq. (22) reduces to:

$$Q_1 = \frac{E_2 \mathrm{EC}_1}{E_1 \mathrm{EC}_2} \quad (23)$$

The fraction of the residual population of constitutively active mutant receptors after reduced receptor expression or partial receptor inactivation with an irreversible inverse agonist (Q_2) is given by:

$$Q_2 = \frac{E_4 \mathrm{EC}_3 (E_3 - B_3)}{E_3 (E_3 \mathrm{EC}_4 - B_3 \mathrm{EC}_3)} \quad (24)$$

Several useful expressions can be derived for the scalar increase in the isomerization constant of the unoccupied receptor caused by the constitutively activating mutation (C_M):

$$C_M = \frac{E_3 (E_3 \mathrm{EC}_1 - B_3 \mathrm{EC}_3)}{B_{\mathrm{max-rel}} E_1 \mathrm{EC}_3 (E_3 - B_3)} \quad (25)$$

$$C_M = \frac{E_4 M_{\mathrm{sys}} (E_3 \mathrm{EC}_1 - B_3 \mathrm{EC}_3)}{B_{\mathrm{max-rel}} E_1 \mathrm{EC}_3 (E_4 M_{\mathrm{sys}} + B_3 (E_4 (Q_2 - 1) - M_{\mathrm{sys}} Q_2))} \quad (26)$$

$$C_M = \frac{E_3 \mathrm{EC}_4 M_{\mathrm{sys}} (E_3 \mathrm{EC}_1 - B_3 \mathrm{EC}_3)}{B_{\mathrm{max-rel}} E_1 \mathrm{EC}_3 (E_3 \mathrm{EC}_4 + B_3 \mathrm{EC}_3)(M_{\mathrm{sys}} + B_3 (Q_2 - 1))} \quad (27)$$

Eq. (29) and one of the three equations described above (i.e., 19–21) can be substituted for Q_2 and M_{sys}, respectively, in Eqs. (26) and (27).

The equation for the active state affinity constant (K_{act}) is given by:

$$K_{\mathrm{act}} = \frac{E_3}{B_3 \mathrm{EC}_3} \quad (28)$$

The equation for the inactive state affinity constant (K_{inact}) is complicated and is described in terms of three main variables (a, b and c) in addition to the previously defined parameters, C_M, K_{act}, M_{sys} and Q_2:

$$K_{\text{inact}}=\frac{a+b}{c} \quad (29)$$

in which,

$$a=K_{\text{act}}E_4(M_{\text{sys}}E_3\text{EC}_1 - B_3E_1\text{EC}_3) \quad (30)$$

$$b=K_{\text{act}}E_1\text{EC}_3(M_{\text{sys}}E_3\text{EC}_1 - B_3E_1\text{EC}_3) \quad (31)$$

$$c=E_4(E_3\text{EC}_1M_{\text{sys}}+E_1\text{EC}_3(B_3(B_{\text{max-rel}} - 1) - M_{\text{sys}}B_{\text{max-rel}})) \quad (32)$$

Alternatively, K_{inact} can be determined using the following substitutions for a, b and c:

$$a=E_1\text{EC}_3B_{\text{max-rel}}(C_M - 1)(M_{\text{sys}}+B_3(Q_2 - 1)) \quad (33)$$

$$b=K_{\text{act}}\text{EC}_4(E_3\text{EC}_1M_{\text{sys}}-E_1\text{EC}_3(B_3+C_MM_{\text{sys}}B_{\text{max-rel}}+B_3(C_M-1)-C_M)B_{\text{max-rel}}) \quad (34)$$

$$c=\text{EC}_4(E_3\text{EC}_1M_{\text{sys}}+E_1\text{EC}_3(B_3(B_{\text{max-rel}} - 1) - M_{\text{sys}}B_{\text{max-rel}})) \quad (35)$$

The equation for the observed isomerization constant of the unoccupied receptor is given by the following equation, which also incorporates previously derived constants:

$$K_{q-\text{obs}}=\frac{K_{\text{inac}}E_4(B_3E_1\text{EC}_3 - E_3\text{EC}_1M_{\text{sys}})+K_{\text{act}}B_3C_ME_1\text{EC}_3Q_2B_{\text{max-rel}}(M_{\text{sys}} - E_4)}{K_{\text{act}}C_M(E_3E_4\text{EC}_1M_{\text{sys}} - B_3E_1\text{EC}_3(Q_2B_{\text{max-rel}}(E_4M_{\text{sys}}) - E_4))}$$

(36)

Finally, the equation for the observed sensitivity constant of the signaling pathway is given by the following equation, which incorporates the previously derived constants, K_q and M_{sys}:

$$K_{E-\mathrm{obs}}=\frac{K_{q-\mathrm{obs}}(E_3\mathrm{EC}_1M_{\mathrm{sys}}-B_3E_1\mathrm{EC}_3)}{B_3E_1\mathrm{EC}_3(1+K_{q-\mathrm{obs}})} \quad (37)$$

A.2. Partial receptor inactivation with an irreversible neutral agonist

The graphical parameters for the case involving partial receptor inactivation with an irreversible neutral antagonist (Fig. 10*b*) are the same as those described above for conditions 1 and 3, but differ for conditions 2 and 4. The graphical parameters for these latter conditions are determined using the strategy described above except that Eq. (5) is used. Again, we follow the same convention for using numerical subscripts (1–4) to identify the four conditions of the assay.

The equations for the E_{max} values for conditions 2 and 4 are given by:

$$E_2=\frac{M_{\mathrm{sys}}K_{q-\mathrm{obs}}(K_{\mathrm{inact}}(1-Q_1)+K_{\mathrm{act}}(K_{q-\mathrm{obs}}+Q_1))}{K_{\mathrm{inact}}(K_{E-\mathrm{obs}}+K_{q-\mathrm{obs}}(K_{E-\mathrm{obs}}+1-Q_1))+K_{\mathrm{act}}K_{q-\mathrm{obs}}(K_{E-\mathrm{obs}}+K_{q-\mathrm{obs}}(K_{E-\mathrm{obs}}+1)+Q_1)}$$

(38)

$$E_4=\frac{M_{\mathrm{sys}}K_{q-\mathrm{obs}}C_MB_{\mathrm{max-rel}}(K_{\mathrm{inact}}(1-Q_2)+K_{\mathrm{act}}(C_MK_{q-\mathrm{obs}}+Q_2))}{K_{E-\mathrm{obs}}(1+K_{q-\mathrm{obs}}C_M)(K_{\mathrm{inact}}+K_{\mathrm{act}}K_{q-\mathrm{obs}}C_M)+K_{q-\mathrm{obs}}C_MB_{\mathrm{max-rel}}(K_{\mathrm{inact}}(1-Q_2)+K_{\mathrm{act}}(C_MK_{q-\mathrm{obs}}+Q_2))}$$

(39)

The equations for the basal response values for conditions 2 and 4 are the same as those for conditions 1 and 3:

$$B_1=B_2=\frac{M_{\mathrm{sys}}K_{q-\mathrm{obs}}}{K_{E-\mathrm{obs}}+K_{q-\mathrm{obs}}(K_{E-\mathrm{obs}}+1)} \quad (40)$$

$$B_3=B_4=\frac{M_{\mathrm{sys}}K_{q-\mathrm{obs}}C_MB_{\mathrm{max-rel}}}{K_{E-\mathrm{obs}}+K_{q-\mathrm{obs}}C_M(K_{E-\mathrm{obs}}+B_{\mathrm{max-rel}})} \quad (41)$$

The equations for the EC_{50} values for conditions 2 and 4 are given by:

$$\mathrm{EC}_2=\frac{(K_{q-\mathrm{obs}}+1)(K_{E-\mathrm{obs}}+K_{q-\mathrm{obs}}(K_{E-\mathrm{obs}}+1))}{K_{\mathrm{inact}}(K_{E-\mathrm{obs}}+K_{q-\mathrm{obs}}(K_{E-\mathrm{obs}}+1-Q_1))+K_{\mathrm{act}}K_{q-\mathrm{obs}}(K_{E-\mathrm{obs}}+K_{q-\mathrm{obs}}(K_{E-\mathrm{obs}}+1)+Q_1)} \quad (42)$$

$$\mathrm{EC}_4=\frac{(K_{q-\mathrm{obs}}C_M+1)(K_E+K_{q-\mathrm{obs}}C_M(K_E+B_{\mathrm{max-rel}}))}{K_E(1+K_{q-\mathrm{obs}}C_M)(K_{\mathrm{inact}}K_{\mathrm{act}}K_{q-\mathrm{obs}}C_M)+K_{q-\mathrm{obs}}C_M B_{\mathrm{max-rel}}(K_{\mathrm{inact}}(1-Q_2)+K_{\mathrm{act}}(C_M K_{q-\mathrm{obs}}+Q_2))} \quad (43)$$

As described in the prior section, these equations together with those for conditions 1 and 3 are solved to yield expressions for the various parameters of the receptor states and transducer function, expressed in terms of the graphical parameters of the concentration-response curves. We begin with the maximal response of the system (M_{sys}), which can be estimated under conditions 1 and 2 or 3 and 4:

$$M_{\mathrm{sys}}=\frac{E_1\mathrm{EC}_2-E_2\mathrm{EC}_1}{\mathrm{EC}_2-\mathrm{EC}_1} \quad (44)$$

$$M_{\mathrm{sys}}=\frac{E_3\mathrm{EC}_4-E_4\mathrm{EC}_3}{\mathrm{EC}_4-\mathrm{EC}_3} \quad (45)$$

The fractions of the residual receptor populations of wild type (Q_1) and mutant (Q_2) receptors after partial inactivation with an irreversible neutral agonist are given by:

$$Q_1=\frac{E_2\mathrm{EC}_1}{E_1\mathrm{EC}_2} \quad (46)$$

$$Q_2=\frac{\mathrm{EC}_3(E_4-B_3)}{\mathrm{EC}_4(E_3-B_3)} \quad (47)$$

The scalar increase in the isomerization constant of the unoccupied receptor caused by the constitutively activating mutation (C_M) is given by Eq. (25) above.

The equation for the active state affinity constant (K_{act}) is given by Eq. (28) above.

The equation for the inactive state affinity constant (K_{inact}) is complicated and is described in terms of five main variables (*a*–e), the previously defined parameter, C_M, and the graphical parameters, E_3, B_3 and EC_3:

$$K_{\text{inact}}=\frac{E_3\left(1-\frac{\text{ab}}{C(d-e)}\right)}{B_3\text{EC}_3} \quad (48)$$

in which,

$$a=(C_M-1)(E_2\text{EC}_1-E_1\text{EC}_2)(E_3\text{EC}_1-B_3\text{EC}_3) \quad (49)$$

$$b=(\text{EC}_3-\text{EC}_4)B_3E_1\text{EC}_3-E_3E_4\text{EC}_1\text{EC}_3+E_3^2\text{EC}_1\text{EC}_4 \quad (50)$$

$$c=C_M(B_3E_1(E_2\text{EC}_1-E_1\text{EC}_2)+B_3E_1(\text{EC}_2-\text{EC}_1)\text{EC}_3) \quad (51)$$

$$d=E_3^2\text{EC}_1\text{EC}_4+E_1\text{EC}_3(E_4\text{EC}_3B_{\text{max-rel}}-B_3(\text{EC}_3-\text{EC}_4)(B_{\text{max-rel}}-1)) \quad (52)$$

$$e=E_3\text{EC}_3(E_4\text{EC}_1+E_1\text{EC}_4B_{\text{max-rel}}) \quad (53)$$

The equation for the isomerization constant of the unoccupied receptor is given by the following equation, which incorporates the previously derived inactive state affinity constant (K_{inact}):

$$K_{q-\text{obs}}=\frac{B_3E_1(E_3\text{EC}_1(E_2-K_{\text{inact}}E_2+\text{EC}_1)+E_1(K_{\text{inact}}E_2-1)+K_{\text{inact}}B_3E_1\text{EC}_3(\text{EC}_1-\text{EC}_2))}{E_3(E_2\text{EC}_1-E_1\text{EC}_2)(E_3\text{EC}_1-B_3\text{EC}_3)}$$

(54)

Finally, the equation for the sensitivity constant of the signaling pathway is given by Eq. (37).

A.3. Validation of equations

To check the validity and robustness of Eqs. (19)–(37) and (44)–(54), we used Eqs. (4) and (5) to generate theoretical data, like those shown in Fig. 1, but having a transducer slope

factor of 1.0 and estimated graphical parameters from the musing a four parameter logistic equation ($y = B + (E - B) / (1 + 10^{(\log EC - \log D)})$). We analyzed data with no error and also data with a 10% Gaussian error as described under Methods. In both cases we were able to estimate accurate receptor-state and system parameters using the equations above and the empirical parameters of the concentration-response curves (i.e., E, EC and B).

Appendix B. Supplementary methods

Supplementary data to this article can be found online at http://dx.doi.org/10.1016/j.vascn.2016.09.007.

References

Auerbach A. The gating isomerization of neuromuscular acetylcholine receptors. The Journal of Physiology. 2010; 588:573–586. [PubMed: 19933754]

Black JW, Leff P. Operational models of pharmacological agonism. Proceedings of the Royal Society of London. Series B: Biological Sciences. 1983; 220:141–162.

Black JW, Leff P, Shankley NP, Wood J. An operational model of pharmacological agonism: The effect of E/[A] curve shape on agonist dissociation constant estimation. British Journal of Pharmacology. 1985; 84:561–571. [PubMed: 3978322]

Bruneau EG, Esteban JA, Akaaboune M. Receptor-associated proteins and synaptic plasticity. The FASEB Journal. 2009; 23:679–688. [PubMed: 18978155]

Chang Y, Weiss DS. Allosteric activation mechanism of the alpha 1 beta 2 gamma 2 gamma-aminobutyric acid type A receptor revealed by mutation of the conserved M2 leucine. Biophysical Journal. 1999; 77:2542–2551. [PubMed: 10545355]

Ehlert, FJ. Ternary complex model. In: Christopoulos, A., editor. Biomedical applications of computer modeling. Boca Raton: CRC Press; 2000. p. 21-85.

Ehlert FJ. On the analysis of ligand directed signaling at G protein coupled receptors. Naunyn-Schmiedeberg's Archives of Pharmacology. 2008; 377:549–577.

Ehlert FJ. Functional studies cast light on receptor states. Trends in Pharmacological Sciences. 2015

Ehlert FJ, Griffin MT. Estimation of ligand affinity constants for receptor states in functional studies involving the allosteric modulation of G protein-coupled receptors: Implications for ligand bias. Journal of Pharmacological and Toxicological Methods. 2014; 69:253–279. [PubMed: 24434717]

Ehlert FJ, Griffin MT, Suga H. Analysis of functional responses at G protein coupled receptors: Estimation of relative affinity constants for the inactive receptor state. The Journal of Pharmacology and Experimental Therapeutics. 2011; 338:658–670. [PubMed: 21576380]

Ehlert FJ, Suga H, Griffin MT. Analysis of agonism and inverse agonism in functional assays with constitutive activity: Estimation of orthosteric ligand affinity constants for active and inactive receptor states. The Journal of Pharmacology and Experimental Therapeutics. 2011; 338:671–686. [PubMed: 21576379]

Ehlert FJ, Griffin MT, Sawyer GW, Bailon R. A simple method for estimation of agonist activity at receptor subtypes: Comparison of native and cloned M3 muscarinic receptors in Guinea pig ileum and transfected cells. The Journal of Pharmacology and Experimental Therapeutics. 1999; 289:981–992. [PubMed: 10215678]

Figueroa KW, Griffin MT, Ehlert FJ. Selectivity of agonists for the active state of M1–M4 muscarinic receptor subtypes. The Journal of Pharmacology and Experimental Therapeutics. 2008; 328:331–342. [PubMed: 18824613]

Furchgott RF. The use of b-haloalkylamines in the differentiation of receptors and in the determination of dissociation constants of receptor-agonist complexes. Advances in Drug Research. 1966; 3:21–55.

Furchgott RF, Bursztyn P. Comparison of dissociation constants and of relative efficacies of selected agonists acting on parasympathetic receptors. Annals of the New York Academy of Sciences. 1967; 144:882–899.

Griffin MT, Figueroa KW, Liller S, Ehlert FJ. Estimation of agonist activity at G protein-coupled receptors: Analysis of M2 muscarinic receptor signaling through Gi/o,Gs, and G15. The Journal of Pharmacology and Experimental Therapeutics. 2007; 321:1193–1207. [PubMed: 17392404]

Guo DF, Sun YL, Hamet P, Inagami T. The angiotensin II type 1 receptor and receptor-associated proteins. Cell Research. 2001; 11:165–180. [PubMed: 11642401]

Guyton JR. Extended-release niacin for modifying the lipoprotein profile. Expert Opinion on Pharmacotherapy. 2004; 5:1385–1398. [PubMed: 15163282]

Guyton JR. Niacin in cardiovascular prevention: Mechanisms, efficacy, and safety. Current Opinion in Lipidology. 2007; 18:415–420. [PubMed: 17620858]

Jencks WP. Binding energy, specificity, and enzymic catalysis: The circe effect. Advances in Enzymology and Related Areas of Molecular Biology. 1975; 43:219–410. [PubMed: 892]

Jha A, Auerbach A. Acetylcholine receptor channels activated by a single agonist molecule. Biophysical Journal. 2010; 98:1840–1846. [PubMed: 20441747]

Kelly E. Efficacy and ligand bias at the mu-opioid receptor. British Journal of Pharmacology. 2013; 169:1430–1446. [PubMed: 23646826]

Kenakin T, Christopoulos A. Signalling bias in new drug discovery: Detection, quantification and therapeutic impact. Nature Reviews. Drug Discovery. 2013; 12:205–216. [PubMed: 23411724]

Kenakin T, Watson C, Muniz-Medina V, Christopoulos A, Novick S. A simple method for quantifying functional selectivity and agonist bias. ACS Chemical Neuroscience. 2012; 3:193–203. [PubMed: 22860188]

Manglik A, Kim TH, Masureel M, Altenbach C, Yang Z, Hilger D, Kobilka BK. Structural insights into the dynamic process of beta2-adrenergic receptor signaling. Cell. 2015; 161:1101–1111. [PubMed: 25981665]

Monod J, Wyman J, Changeux JP. On the nature of allosteric transitions: A plausible model. Journal of Molecular Biology. 1965; 12:88–118. [PubMed: 14343300]

Nygaard R, Zou Y, Dror RO, Mildorf TJ, Arlow DH, Manglik A, Kobilka BK. The dynamic process of beta(2)-adrenergic receptor activation. Cell. 2013; 152:532–542. [PubMed: 23374348]

Rasmussen SG, Choi HJ, Rosenbaum DM, Kobilka TS, Thian FS, Edwards PC, Kobilka BK. Crystal structure of the human beta2 adrenergic G-protein-coupled receptor. Nature. 2007; 450:383–387. [PubMed: 17952055]

Rasmussen SG, DeVree BT, Zou Y, Kruse AC, Chung KY, Kobilka TS, Kobilka BK. Crystal structure of the beta2 adrenergic receptor-Gs protein complex. Nature. 2011; 477:549–555. [PubMed: 21772288]

Richman JG, Kanemitsu-Parks M, Gaidarov I, Cameron JS, Griffin P, Zheng H, Connolly DT. Nicotinic acid receptor agonists differentially activate downstream effectors. The Journal of Biological Chemistry. 2007; 282:18028–18036. [PubMed: 17452318]

Ruiz de Azua I, Nakajima K, Rossi M, Cui Y, Jou W, Gavrilova O, Wess J. Spinophilin as a novel regulator of M3 muscarinic receptor-mediated insulin release in vitro and in vivo. The FASEB Journal. 2012; 26:4275–4286. [PubMed: 22730439]

Spalding TA, Burstein ES, Wells JW, Brann MR. Constitutive activation of the m5 muscarinic receptor by a series of mutations at the extracellular end of transmembrane 6. Biochemistry. 1997; 36:10109–10116. [PubMed: 9254607]

Staus DP, Strachan RT, Manglik A, Pani B, Kahsai AW, Kim TH, Lefkowitz RJ. Allosteric nanobodies reveal the dynamic range and diverse mechanisms of G-protein-coupled receptor activation. Nature. 2016; 535:448–452. [PubMed: 27409812]

Stein RS, Ehlert FJ. A kinetic model of GPCRs: Analysis of G protein activity, occupancy, coupling and receptor-state affinity constants. Journal of Receptor and Signal Transduction Research. 2015; 35:269–283. [PubMed: 25353707]

Tran JA, Chang A, Matsui M, Ehlert FJ. Estimation of relative microscopic affinity constants of agonists for the active state of the receptor in functional studies on M2 and M3 muscarinic receptors. Molecular Pharmacology. 2009; 75:381–396. [PubMed: 18996972]

Walters RW, Shukla AK, Kovacs JJ, Violin JD, DeWire SM, Lam CM, Lefkowitz RJ. Beta-Arrestin1 mediates nicotinic acid-induced flushing, but not its antilipolytic effect, in mice. The Journal of Clinical Investigation. 2009; 119:1312–1321. [PubMed: 19349687]

Whalen EJ, Rajagopal S, Lefkowitz RJ. Therapeutic potential of beta-arrestin- and G protein-biased agonists. Trends in Molecular Medicine. 2011; 17:126–139. [PubMed: 21183406]

Ye L, Van Eps N, Zimmer M, Ernst OP, Prosser RS. Activation of the A2A adenosine G-protein-coupled receptor by conformational selection. Nature. 2016; 533:265–268. [PubMed: 27144352]

Zhang R, Kavana M. Quantitative analysis of receptor allosterism and its implication for drug discovery. Expert Opinion on Drug Discovery. 2015; 10:763–780. [PubMed: 25927503]

Zhang R, Kavana M. Quantitative measure of receptor agonist and modulator equi-response and equi-occupancy selectivity. Scientific Reports. 2016; 6:25158. [PubMed: 27116909]

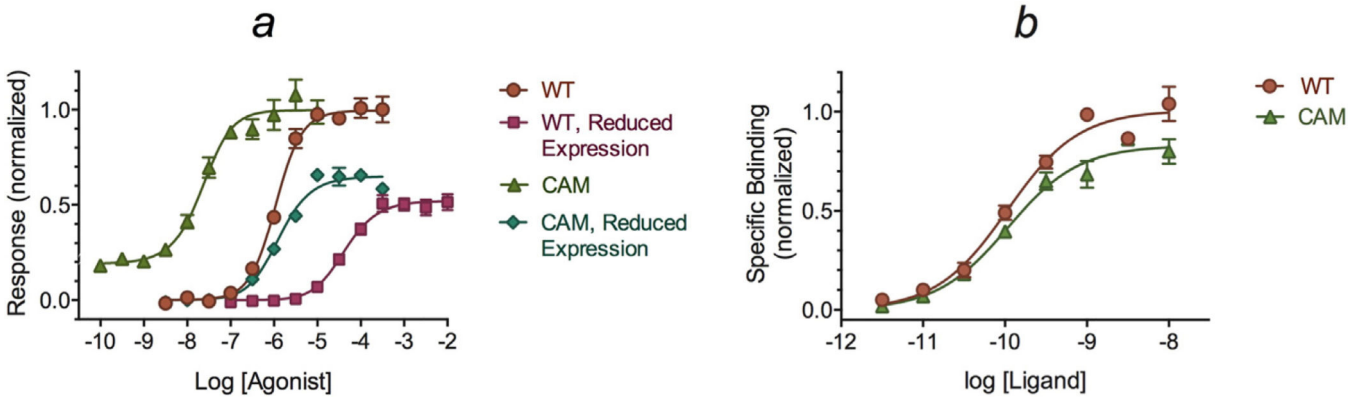

Fig. 1.

Simulation of the agonist responses and ligand binding properties of a wild type receptor and a constitutively active mutant of it. *a*, Simulation of agonist concentration-response curves for a response mediated by wild type and constitutively receptors under conditions of control and reduced levels of receptor expression. *b*, Simulation of the binding of radioligand to the wild type and constitutively active receptor populations that elicited the responses shown in *a*. The curves represent the least-squares fit of Eqs. (4) and (6) to the simulated data shown in panels *a* and *b*, respectively. The data points represent the mean values ± SEM of four simulations. The parameter values used for the simulation are listed in Table 2.

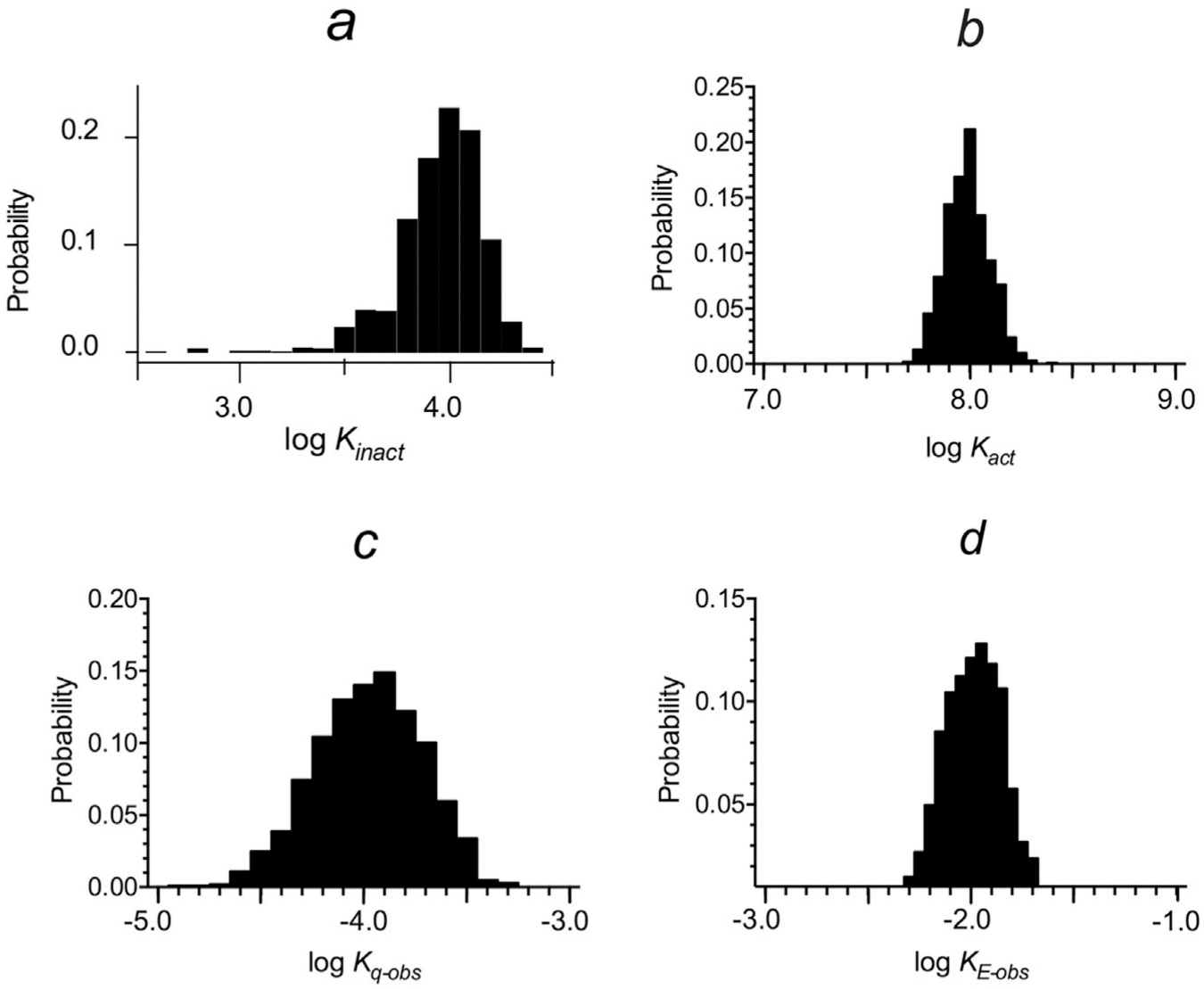

Fig. 2.

Probability density functions for the mean log estimates of K_{inact} (*a*), K_{act} (*b*), $K_{q\text{-}obs}$ (c) *and* $K_{E\text{-}obs}$ (*d*). A Monte Carlo analysis, consisting of 1020 simulations, was carried out for the parametric conditions illustrated in Fig. 1. The plots show the probability density functions for the 1007 simulations for which values of log $K_{inact} > 0$ were obtained.

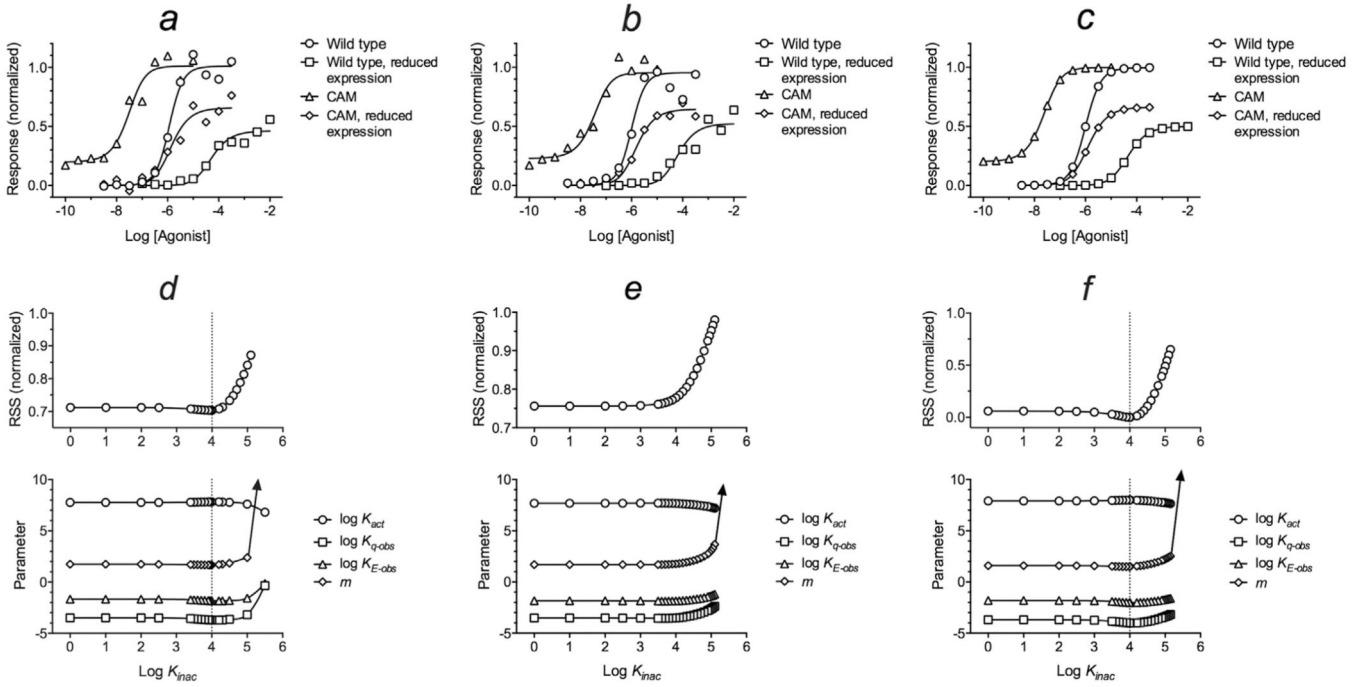

Fig. 3.

Nonlinear regression analysis of simulated data with Gaussian error (*a* and *b*) and no error (*c*). The simulated data shown in panels *a* and *b* represent the results of a single simulation each. The simulated data in panels *a*, *b* and *c* were analyzed by nonlinear regression analysis (Eq. (4)) with the value of log K_{inact} constrained to various values indicated on the abscissas of the upper plots shown in panels *d*, *e* and *f*, respectively. These latter plots show the value of the residual sum of squares (*RSS*) plotted against the value to which log K_{inact} was constrained during the regression. Only in cases *d* and *f* was the least-squares fit associated with a unique estimate of log K_{inact}. The lower panels in in *d*, *e* and *f* show the corresponding values of the parameters, log K_{act}, log $K_{q\text{-}obs}$, log $K_{E\text{-}obs}$ and *m*.

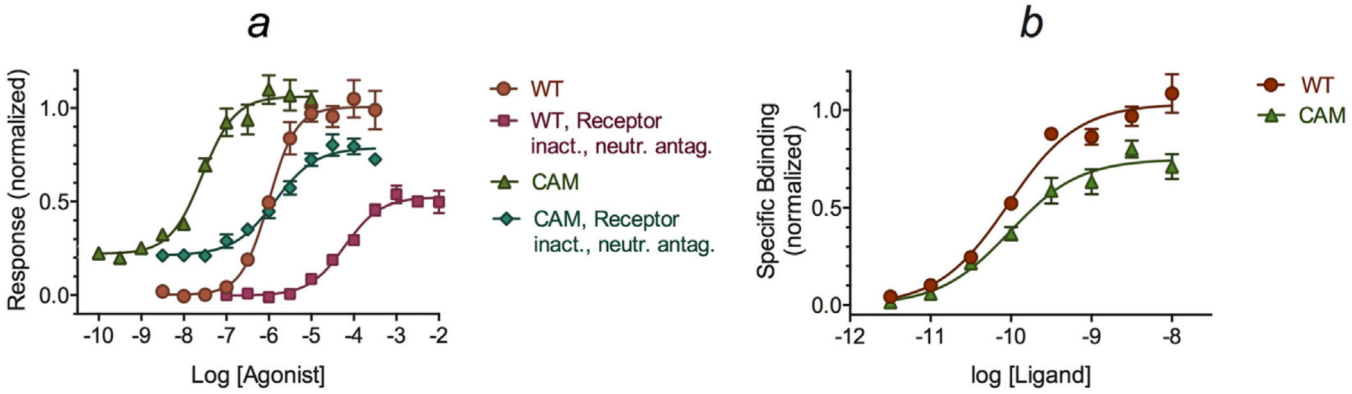

Fig. 4.

Simulation of the agonist response and ligand binding properties of a wild type receptor and a constitutively active mutant of it. *a*, Simulation of agonist concentration-response curves for a response mediated by wild type and constitutively receptors under conditions of control and partial receptor inactivation with an irreversible neutral antagonist. *b*, Simulation of the binding of radioligand to the wild type and constitutively active receptor populations that elicited the responses shown in *a*. The curves represent the least-squares fit of Eqs. (5) and (6) to the simulated data shown in panels *a* and *b*, respectively. The data points represent the mean values ± SEM of four simulations. The parameter values used for the simulation are listed in Table 2.

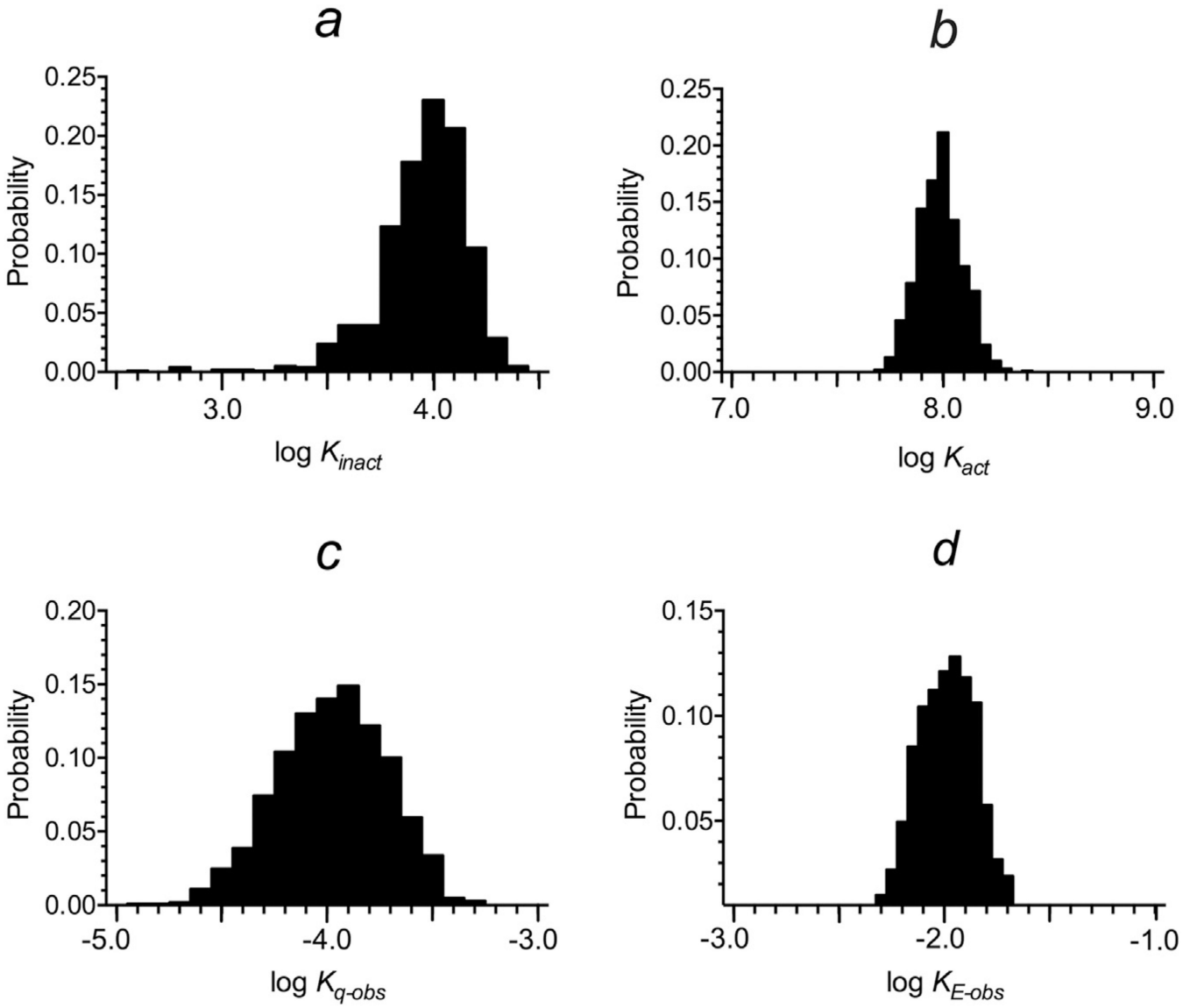

Fig. 5.

Probability density functions for the mean log estimates of K_{inact} (*a*), K_{act} (*b*), $K_{q\text{-}obs}$ (c) *and* $K_{E\text{-}obs}$ (*d*). A Monte Carlo analysis, consisting of 150 simulations, was carried out for the parametric conditions illustrated in Fig. 4. The plots show the probability density functions for the 149 simulations for which values of log $K_{inact} > 0$ were obtained.

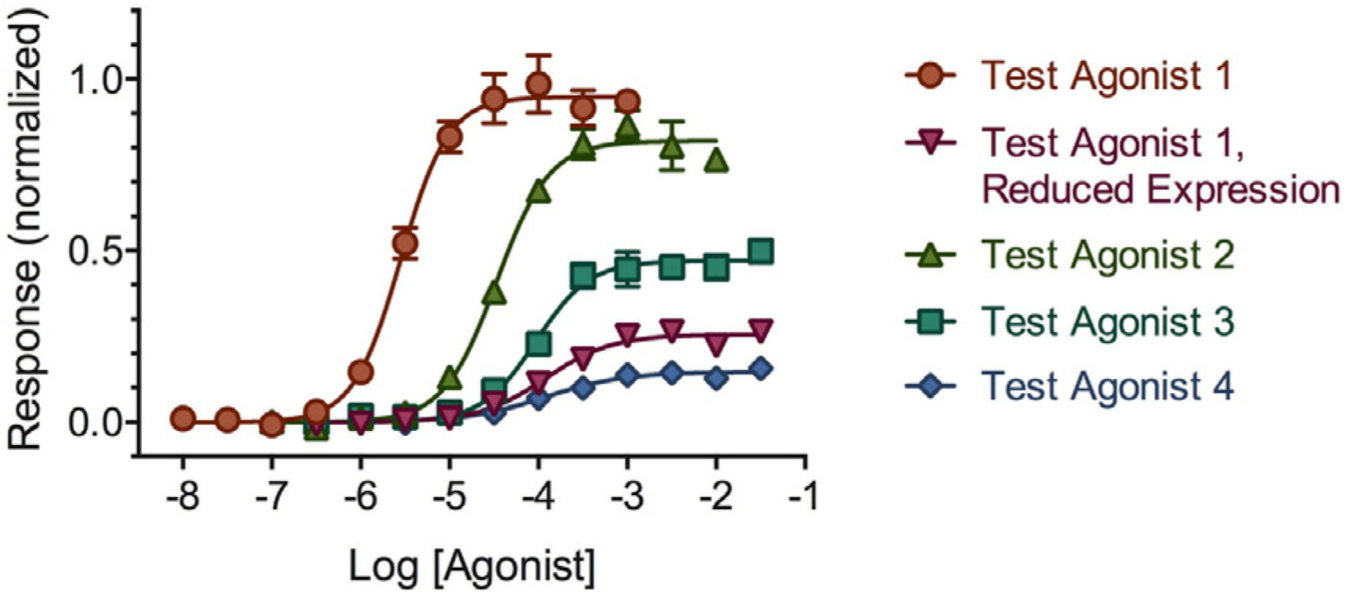

Fig. 6.

Simulation of the response of a wild type receptor in the presence of various test agonists (1–4). Efficacious test agonist 1 was also simulated for the condition of partial receptor inactivation. The simulated data were analyzed simultaneously with those shown in Figs. 1 and 4. The curves represent the least-squares fit of Eqs. (4) or (5) to the data depending, on whether the analysis included the data from Figs. 1 or 4, respectively. The data points represent the mean values ± SEM of four simulations. The parameter values used for the simulation are listed in Table 3.

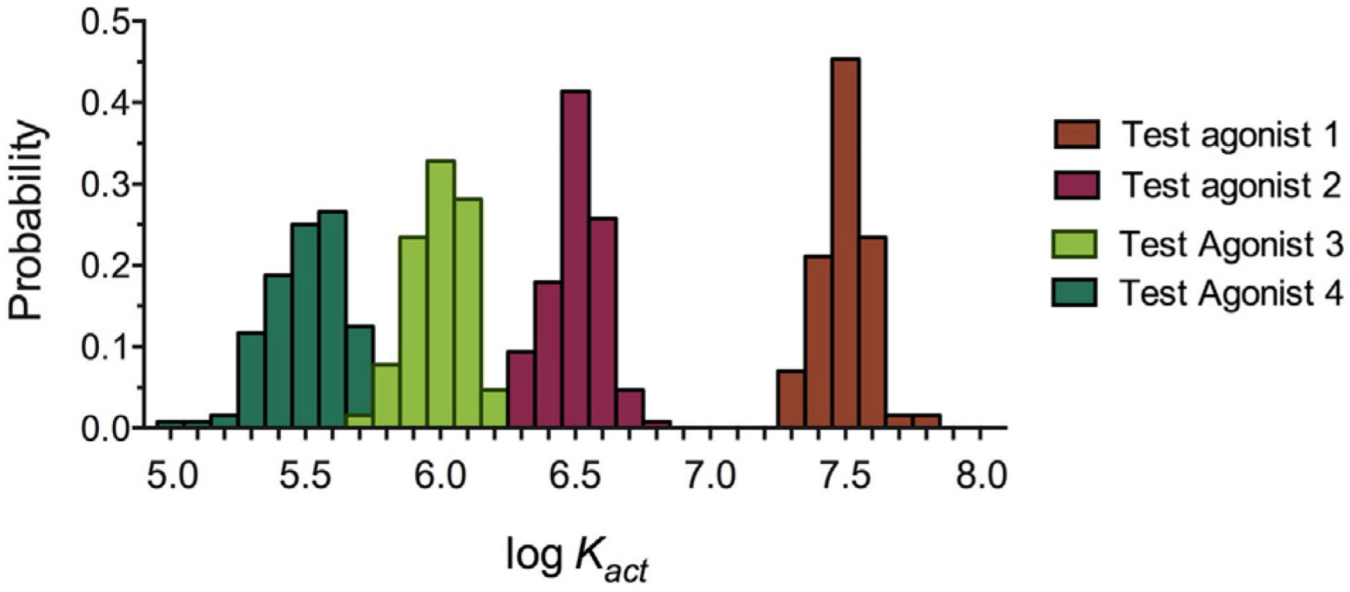

Fig. 7.

Probability density functions for the mean log estimates of K_{act} for the test agonists illustrated in Fig. 6. A Monte Carlo analysis, consisting of 127 simulations, was carried out for the parametric conditions illustrated in Fig. 6. The plots shows the probability density functions for the estimates of log K_{act} for test agonists 1–4.

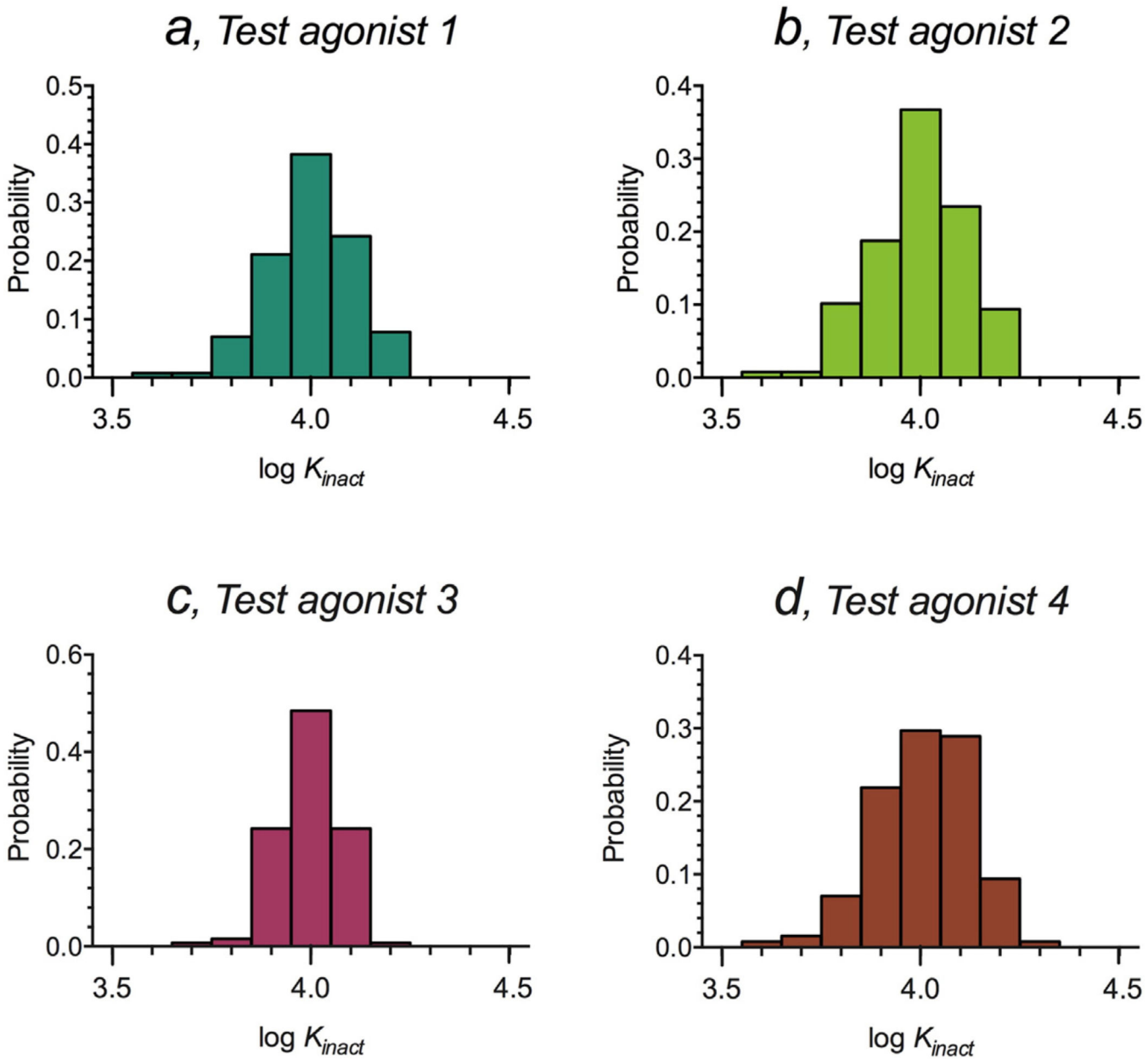

Fig. 8.

Probability density functions for the mean log estimates of K_{inact} for the test agonists illustrated in Fig. 6. A Monte Carlo analysis, consisting of 127 simulations, was carried out for the parametric conditions illustrated in Fig. 6. The plots shows the probability density functions for the estimates of log K_{inact} for test agonists 1–4.

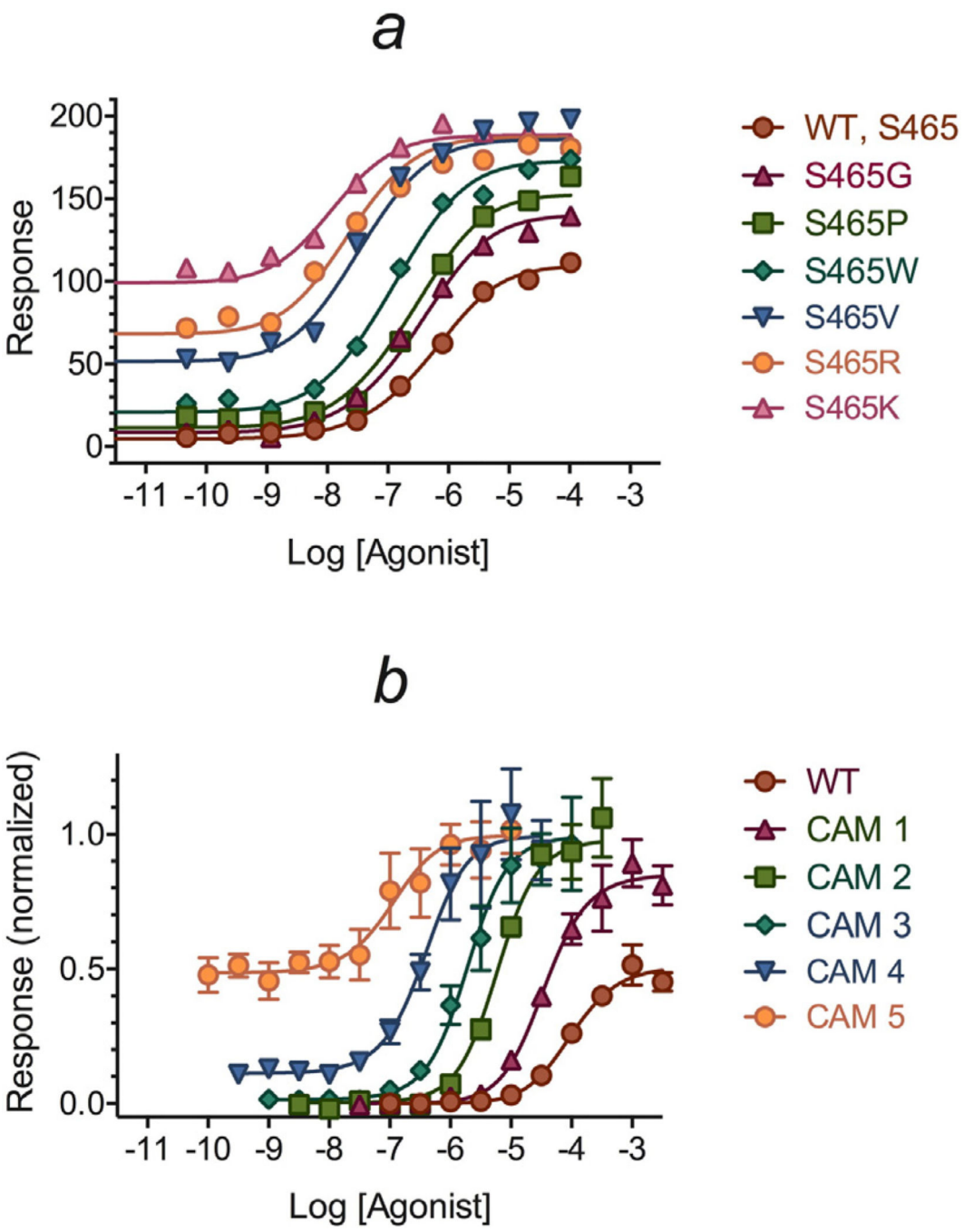

Fig. 9.

Analysis of the responses of a wild type receptor and several constitutively active mutants of it. *a*, The published data of Spalding et al. (1997) from Fig. 7 of their manuscript. The data points represent mean values of 2–4 experiments. *b*, Simulated data. The plot shows means ± SEM from four simulations. The theoretical curves represents the least-squares fit of Eq. (4) to the data.

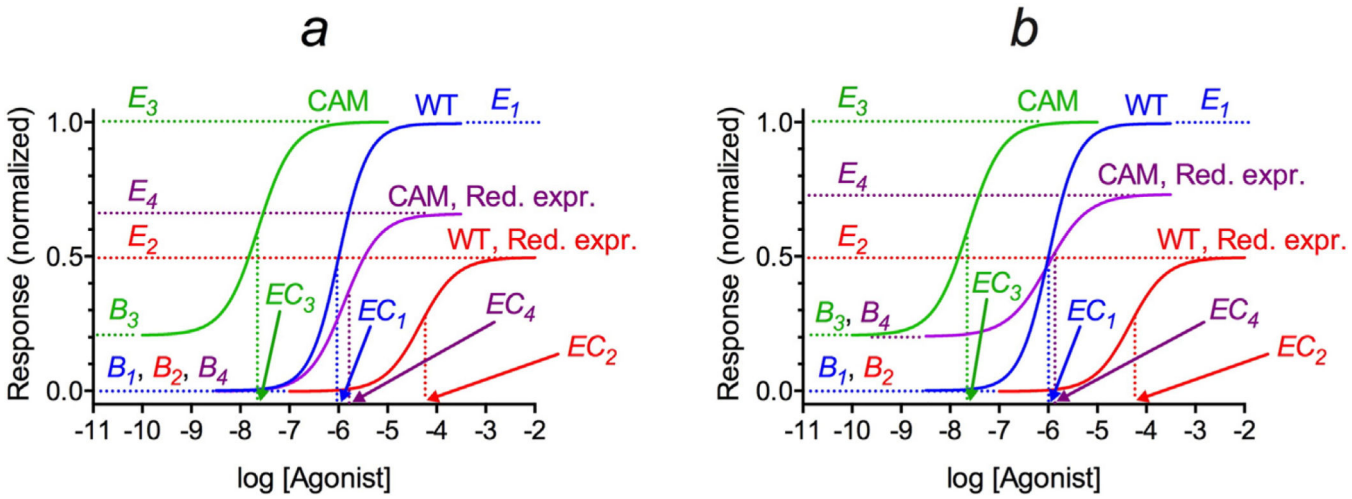

Fig. 10.

Graphical parameters of agonist concentration-response curves for protocols involving reduced-receptor expression (a) or partial receptor inactivation with an irreversible neutral antagonist (b). The protocol illustrated in panel *a* also applies to partial receptor inactivation with an irreversible inverse agonist. Abbreviations used: CAM, constitutively active receptor mutant; WT, wild type; Red. expr., reduced expression; E, maximal response; EC, EC_{50} and B, constitutive response in the absence of agonist. (For interpretation of the references to colour in this figure legend, the reader is referred to the web version of this article.)

Table 1

Parameters used in nonlinear regression analysis[a].

Parameter	Definition
Receptor states	
K_{act}	Active state affinity constant (units, M^{-1})
K_{inact}	Inactive state affinity constant (units, M^{-1})
$K_{q\text{-}obs}$	Observed isomerization constant. Its value is perturbed from that of the isolated receptor (K_q) by G protein and guanine nucleotides.
Transducer function	
M_{sys}	The maximum of the output response for an agonist with an infinite K_{act}/K_{inact} ratio
K_E	Sensitivity constant of the transducer function (units, receptor concentration, R_T)
m	Transducer slope factor
Composite	
$K_{E\text{-}obs}$	$\frac{K_E}{R_T T_{\max}}$, T_{max} denotes maximal efficacy of an agonist with an infinite K_{act}/K_{inact} ratio
RA_i	Estimate of K_{act}, expressed relative to that of a standard agonist (K_{act}')

[a]The relationship between the above receptor state parameters and the more conventional population parameters are described in Ehlert and Griffin (2014).

Table 2

Summary of nonlinear regression analysis of the simulated data in Figs. 1 and 4.

Parameter	Fig. 1	Fig. 4	Value used in simulation
log K_{act}	8.03 ± 0.058	8.04 ± 0.20	8.0
log K_{inact}	4.03 ± 0.15	3.87 ± 0.25	4.0
log $K_{q\text{-}obs}$	−4.03 ± 0.055	−4.37 ± 0.36	−4.0
log $K_{E\text{-}obs}$	−1.97 ± 0.023	−2.23 ± 0.10	−2.0
log C_M	1.73 ± 0.040	1.79 ± 0.14	1.70
q_{WT}	0.025 ± 0.0025	0.018 ± 0.007	0.02
q_M	0.020 ± 0.0017	0.015 ± 0.001	0.02
M_{sys}	1.00 ± 0.016	1.065 ± 0.055	1.00
m	1.53 ± 0.050	1.52 ± 0.43	1.50
log $K_{D\text{-}WT}$	−10.04 ± 0.040	−10.04 ± 0.026	−10.0
log $K_{D\text{-}M}$	−9.80 ± 0.057	−10.00 ± 0.058	−10.0
$B_{max\text{-}WT}$	1.01 ± 0.040	1.034 ± 0.030	1.0
$B_{max\text{-}rel}$	0.84 ± 0.055	0.73 ± 0.016	0.80

Table 3

Summary of nonlinear regression analysis of the simulated data in Figs. 1,4 and 6.

Parameter	Figs. 1 & 6	Figs. 4 & 6	Value used in simulation
Standard agonist			
log K_{act}	7.99 ± 0.056	8.05 ± 0.097	8.0
log K_{inact}	4.06 ± 0.16	3.96 ± 0.14	4.0
Test agonist 1			
log K_{act}	7.55 ± 0.057	7.53 ± 0.12	7.5
log K_{inact}	4.13 ± 0.10	3.91 ± 0.07	4.0
Test agonist 2			
log K_{act}	6.55 ± 0.046	6.55 ± 0.076	6.5
log K_{inact}	4.06 ± 0.032	3.92 ± 0.13	4.0
Test agonist 3			
log K_{act}	6.05 ± 0.057	5.92 ± 0.05	6.0
log K_{inact}	4.04 ± 0.021	3.83 ± 0.12	4.0
Test agonist 4			
log K_{act}	5.75 ± 0.14	5.33 ± 0.07	5.5
log K_{inact}	4.21 ± 0.11	3.82 ± 0.07	4.0
Additional parameters			
log $K_{q\text{-}obs}$	−3.95 ± 0.076	−4.39 ± 0.13	−4.0
log $K_{E\text{-}obs}$	−1.94 ± 0.043	−2.29 ± 0.07	−2.0
log C_M	1.72 ± 0.049	1.78 ± 0.073	1.70
q_{WT}	0.027 ± 0.004	0.016 ± 0.0022	0.02
q_M	0.022 ± 0.002	0.014 ± 0.0017	0.02
M_{sys}	0.98 ± 0.009	1.05 ± 0.032	1.00
m	1.64 ± 0.038	1.35 ± 0.12	1.50
log $K_{D\text{-}WT}$	−9.97 ± 0.047	−10.04 ± 0.025	−10.0
log $K_{D\text{-}M}$	−9.96 ± 0.079	−10.00 ± 0.053	−10.0
$B_{max\text{-}WT}$	1.01 ± 0.038	1.032 ± 0.029	1.0
$B_{max\text{-}rel}$	0.83 ± 0.054	0.73 ± 0.016	0.80

Table 4

Protocols for estimating receptor-state and system parameters

This table identifies what receptor-state and system parameters can be estimated in experiments on cells expressing wild type and constitutively active mutant (CAM) receptors. The protocols differ with respect to whether or not agonist responses are measured under conditions of a reduced density of accessible receptors (RDAR) (i.e., reduced receptor expression or partial receptor inactivation with an irreversible neutral antagonist or inverse agonist).

	Parameter						
Protocol[a]	K_{act}	K_{inact}	$K_{q\text{-}obs}$	$K_{E\text{-}obs}$	M_{sys}	m	τ_{sys}[b]
#1, full agonist	+	+	+	+	+	+	+
partial agonist	+	+	+	+	+	+	+
#2, full agonist	+				+	+	+
partial agonist	+	+			+	+	+
#3, full agonist	+		+	+	+	+	+
partial agonist	+	+	+	+	+	+	+
#4, full agonist	+				+	+	+
partial agonist	+	+			+	+	+

[a] The protocol number refers to the set of cellular receptor populations used for measuring agonist concentration-response curves: Protocol #1, Wild type, control and RDAR; CAM, control and RDAR. Protocol #2, Wild type, control and RDAR; CAM, control. Protocol #3,Wild type, control; CAM, control and RDAR. Protocol #4,Wild type, control; CAM, control.

[b] The parameter, τ_{sys}, is equivalent to $K_{q\text{-}obs}/(K_{E\text{-}obs}(1 + K_{q\text{-}obs}))$.